

1 **Title**

2 **Inhibition of Extracellular Vesicle-Associated MMP2 Abrogates Intercellular Transfer**  
3 **of Hepatic miR-122 to Tissue Macrophages and Curtails Liver Inflammation**

4 **Running Title**

5 MMP2 control EV-movement in intercellular space

6 **Authors**

7 Arnab Das<sup>1#</sup>, Sudarshana Basu<sup>1#</sup>, Diptankar Bandyopadhyay<sup>1</sup>, Debduiti Dutta<sup>1</sup>, Sreemoyee  
8 Chakrabarti<sup>1</sup>, Moumita Adak<sup>2</sup> Snehasikta Swarnakar<sup>3</sup>, Partha Chakrabarti<sup>2</sup>, and Suvendra N.  
9 Bhattacharyya<sup>1,\*</sup>

10 <sup>1</sup>RNA Biology Research Laboratory, Molecular Genetics Division, CSIR-Indian Institute of  
11 Chemical Biology

12 <sup>2</sup> Cell Biology and Physiology Division, CSIR-Indian Institute of Chemical Biology

13 <sup>3</sup> Infectious Diseases and Immunology Division, CSIR-Indian Institute of Chemical Biology

14 \*Corresponding Author

15 # Both authors contributed equally

16 Address of correspondence: CSIR-Indian Institute of Chemical Biology, 4 Raja S C Mullick  
17 Road, Kolkata 700032, India

18 email: [suvendra@iicb.res.in](mailto:suvendra@iicb.res.in)

19

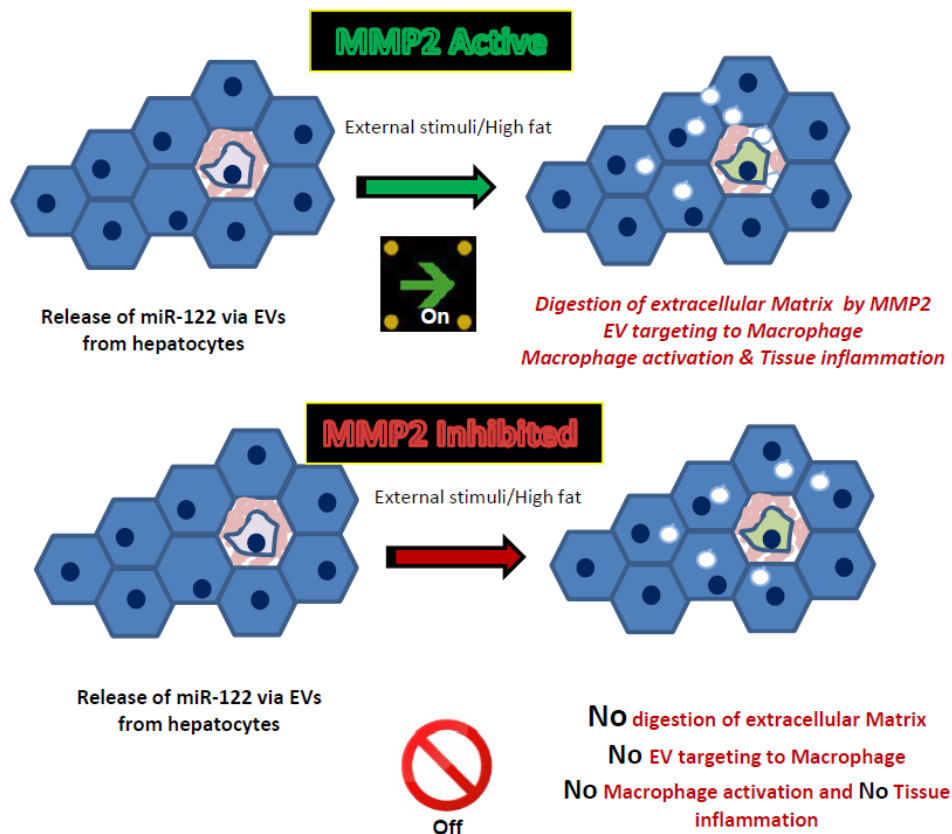
20

## Abstract

21  
22  
23  
24  
25  
26  
27  
28  
29  
30  
31  
32  
33  
34  
35  
36  
37  
38  
39

microRNA-122 (miR-122), a liver specific regulatory RNA, plays an important role in controlling metabolic homeostasis in mammalian liver cells. Interestingly, miR-122 is also a proinflammatory microRNA and when exported to tissue resident macrophage induces expression of inflammatory cytokines there. We found intercellular transfer of miR-122 in lipid exposed liver plays a role in liver inflammation. Exploring the mechanism of intercellular miR-122 transfer from hepatic cells, we detected MMP2 on the membrane of extracellular vesicles derived from hepatic cells which proved to be essential for transfer of extracellular vesicles and their miRNA content from hepatic to non-hepatic cells. Matrix metalloproteinase 2 or MMP2 is a metalloproteinase that plays a key role in shaping and remodelling the extracellular matrix of human tissue by targeting degradation of matrix proteins. MMP2 was found to increase the movement of the EVs along the extracellular matrix to enhance their uptake in recipient cells. Inhibition of MMP2 restricts functional transfer of hepatic miRNAs across the hepatic and non-hepatic cell boundaries. By targeting MMP2, we could reduce the innate immune response in mammalian liver by preventing intra-tissue miR-122 transfer.

**Keywords:** miRNA; EV-mediated miRNA transfer; Liver inflammation; Matrix metalloproteinase; cytokines; High fat diet induced tissue inflammation



40

41

42

43

44

45

46

47

48

49

- Human hepatocytes on exposure to high lipid export out miRNAs including proinflammatory miR-122.
- Extracellular miR-122 is taken up by tissue macrophages to get them activated to produce inflammatory cytokines.
- MMP2 present on the surface of the EVs released by hepatocyte is essential for miRNA transfer to macrophage cells
- Inhibition of MMP2 prevents miR-122 transfer to macrophage and stops activation of recipient macrophage.

## Introduction

50  
51  
52  
53  
54  
55  
56  
57  
58  
59  
60  
61  
62  
63  
64  
65  
66  
67  
68  
69  
70  
71  
72  
73  
74  
75

miRNAs are 22 nt long regulatory RNAs that can repress protein synthesis from their target mRNAs by imperfect base pairing (Bartel, 2018; Filipowicz et al, 2008). Majority of mammalian genes are under miRNA regulation and deregulation of miRNA activity and expression is associated with human diseases (Bartel, 2009). These tiny regulatory RNAs that primarily affect the post-transcriptional steps of gene expression can also be transferred across cell boundaries. Extracellular vesicle (EV) or exosome mediated delivery of miRNA acts as a major way of exchange of genetic information between cells in mammalian tissues and organs (Valadi et al, 2007). The pathology of different diseases is found to be associated with deregulation of miRNA machineries including its export via EVs. Export of miRNAs via EVs thus, not only plays a critical role in maintaining the homeostasis of gene expression in higher eukaryotes but also allows rapid response by recipient cells under stress (Mukherjee et al, 2016).

Hepatic miRNA., miR-122, identified as a highly abundant liver-specific miRNA, has a significant role in controlling hepatic metabolic processes (Chang et al, 2004). Inhibition of miR-122 leads to down-regulation of a number of lipogenic and cholesterol biosynthesis genes in the liver (Esau et al, 2006; Jopling, 2012). This in turn leads to reduced plasma cholesterol, increased hepatic fatty-acid oxidation and reduced synthesis of hepatic lipids. Various studies on circulating miRNAs in NAFLD patients reveal a distinctive serum miRNA profile based on the progression of disease. Upregulated levels of miR-122, miR-192 and miR-375 could be correlated with disease severity in NASH patients as compared to patients with steatosis only (Pirola et al, 2015).

The extracellular vesicles or exosomes are 30-100 nm diameter particles and presence of specific proteins and RNA cargo within the EVs make them unique and cell type specific and thus selectively get delivered to target cells where cell-type specific uptake occurs either by receptor mediated endocytosis or phagocytic activity of the recipient cells.

76 EV-entrapped miRNAs are also secreted into the extracellular milieu (blood, serum or  
77 plasma) and circulating miRNAs, being identified as potential biomarkers for metabolic  
78 diseases, can act as paracrine and endocrine signals in circulation, and can influence the  
79 target gene expression in recipient cells (Basu & Bhattacharyya, 2014; Wang et al, 2019).  
80 Recently, a study showed that in alcohol fed mice, miRNA-122 transferred via Extracellular  
81 Vesicles (EVs) to monocytes and liver Kupffer cells sensitized them to LPS stimulation and  
82 pro-inflammatory cytokine production (Momen-Heravi et al, 2015).

83 How the EVs with their cargo get transferred through the extracellular matrix before  
84 they get delivered to recipient cells is an interesting question and the matrix  
85 metalloproteases are interesting candidates to explore (Shimoda & Khokha, 2017). Recently,  
86 MMP2 has been identified as a metalloprotease present in the EV released by osteoblast  
87 cells and found to be essential for endothelial cell angiogenesis (Tang et al, 2019). MMP2  
88 has been found to be recruited to membranes via MMP14 that is known to act as an adopter  
89 protein of MMP2 for its association with biomembranes (Han et al, 2015). MMP2 in its  
90 mature form is an abundant matrix metalloprotease and its level in the matrix is heavily  
91 regulated and found to be altered in liver disease context (Wang et al, 2014). In different  
92 types of cancers the importance of MMP2 is well documented (Han et al, 2020).

93 In this manuscript, we have documented the presence of MMP2 in the EVs isolated  
94 from hepatic cells. The EV association of MMP2 is MMP14 dependent and we have also  
95 noted that the EVs with MMP2 can ensure functional cell to cell miRNA transfer. This  
96 process is blocked by the MMP2 inhibitor and restored by recombinant MMP2. The transfer  
97 of pro-inflammatory miR-122 from hepatocytes to liver resident macrophage cells is  
98 dependent on MMP2. We have also documented the retardation of movement of EVs in  
99 collagen matrix by MMP2 inhibitor. Thus MMP2 can facilitate the functional miRNA cargo  
100 transfer across cell boundaries via EVs and by blocking the EV-transport with MMP2  
101 inhibitor the expression of inflammatory cytokines can be perturbed in mammalian liver.

103  
104  
105  
106  
107  
108  
109  
110  
111  
112  
113  
114  
115  
116  
117  
118  
119  
120  
121  
122  
123  
124  
125  
126  
127  
128

## Results

### Transfer of hepatic miR-122 to recruited monocytes and Kupffer cells in Methionine Choline Deficient (MCD) diet fed mice livers

Obesity is known to be accompanied by a low grade, chronic inflammatory response orchestrated by pro-inflammatory cytokines like IL-1 $\beta$ , TNF- $\alpha$ , IL-6, CCL2 and others (Berg & Scherer, 2005; Shoelson et al, 2006). The liver is also a site for inflammation in the obese state (Cai et al, 2005). Macrophages are known to play a significant role in hepatic inflammation and subsequent development of insulin resistance (Alisi et al, 2017). The hepatic macrophage population is a heterogenous one, composed of resident Kupffer cells (KC) and infiltrating macrophages (Recruited Hepatic Macrophages-RHM). We wanted to explore the importance of liver specific miRNAs in activation of tissue macrophages on exposure to MCD diet. To address this point, we chose to study a mice model of NASH by feeding the mice with MCD diet for 30 days (Caballero et al, 2010) and FACS sorting the two macrophage populations by differentially labelling them with fluorescent markers (Figure 1A). MCD diet fed mice livers showed increased fat accumulation and hepatocyte ballooning characteristic of NASH (Figure 1B). Normal chow (Ch) fed mice livers show none of these characteristics of NASH. Non-Parenchymal cells were isolated from hepatic cell suspensions prepared from both MCD and Chow diet fed mice livers followed by FACS sorting of F4/80<sup>+</sup>/CD11b<sup>+</sup> dual marker positive KC cells (R5) and F4/80<sup>low</sup>/CD11b<sup>+</sup> RHM cells that have low expression of F4/80 (R4) (Figure 1A) (Morinaga et al, 2015). The F4/80<sup>low</sup>/CD11b<sup>+</sup> set (R4) was sorted out as this represents fresh RHMs derived from circulating monocytes (Morinaga et al, 2015). The CD11b<sup>+</sup> population in MCD diet fed mice livers appeared as two discrete fractions- the F4/80<sup>low</sup>/CD11b<sup>+</sup> set (R4) and the F4/80<sup>high</sup>/CD11b<sup>+</sup> set (R8). R8 appeared to be negligible in Ch diet fed mice and probably represents matured differentiated macrophages and was not included in the analysis (Morinaga et al, 2015). We restricted our

129 investigations to the R4 population as they represent fresh RHM and hence would be more  
130 representative of conditions leading to infiltration and inflammation (Morinaga et al, 2015).

131 RT-qPCR analysis of RNA from isolated RHM (R4- F4/80<sup>low</sup>/CD11b<sup>+</sup> set) showed higher  
132 levels of hepatic miR-122 in RHM of MCD diet fed mice livers as compared to those isolated  
133 from Chow diet fed mice (Figure 1C; upper panel). However levels of miR-16, another  
134 hepatic miRNA known to be present in circulation (Tan et al, 2014), remained unchanged  
135 (Figure 1C; lower panel). We also checked levels of precursor miR-122 levels in RHM to  
136 verify that miR-122 was not being endogenously induced to be expressed in the sorted RHM  
137 cells and was neither contributed by contamination from miR122 expressing hepatic cells  
138 (Figure 1C; middle panel). Equivalent results were obtained for KC (R5- F4/80<sup>+</sup>/CD11b<sup>+</sup>)  
139 cells sorted from Chow and MCD diet fed mice livers. Cells from MCD diet fed mice show  
140 significantly elevated levels of hepatic miR-122 (Figure 1D; upper left panel), whereas  
141 changes in miR-16 levels were found to be non-significant (Figure 1D; upper right panel).  
142 Sorted KC cells also do not induce transcription of pre-miR-122 as verified by decreased  
143 levels of precursor miR-122 in MCD diet fed mice as compared to Chow diet (Figure 1D,  
144 lower left panel). Interestingly, in the sorted KC cells there was an upregulation of miR-155,  
145 an inflammatory miRNA (Figure 1D, lower right panel).

146 Relative quantification of pro-inflammatory cytokine mRNAs was compared between  
147 control (Chow diet fed Mice) and MCD diet fed group. Internalization of miR-122 correlated  
148 with increased levels of IL-6 and IL-1 $\beta$  in RHM (F4/80<sup>low</sup>/CD11b<sup>+</sup>) from MCD diet fed mice  
149 livers (Figure 1E). Similar increases in TNF $\alpha$ , IL-6 and IL-1 $\beta$  levels were detected in KC  
150 (F4/80<sup>+</sup>/CD11b<sup>+</sup> cells) cells (Figure 1F). Thus, both tissue resident KCs and recruited  
151 monocytes from circulation are in an inflammatory state in the obese liver where elevated  
152 presence of hepatic miR-122 was noted.

153 **Induction of inflammatory cytokines in tissue resident macrophages is caused by**  
154 **increased transfer of hepatic miR-122**

155 How does the liver derived miR-122 increase in tissue resident macrophages? We wanted to  
156 investigate the role of lipid exposed liver cell derived extracellular vesicles (EVs) in the  
157 induction of inflammation of receiving macrophages. Huh7 is a human hepatoma cell known  
158 to express miR-122. These cells, when exposed to a cholesterol-lipid concentrate present in  
159 the culture medium for 4 hours, were found to export miR-122. EVs isolated from Huh7 cells  
160 (Basu and Bhattacharyya, 2014) were examined for their miRNA content (Figure 2B). As  
161 expected we detected increased levels of miR-122 there. Three other miRNAs, miR-16, miR-  
162 24 and miR-21 also showed increased levels in EVs isolated from cholesterol treated cells.  
163 miR-16 does show a relatively lower change in its level in released EVs after cholesterol  
164 exposure (Figure 2B). To test whether the EVs isolated from hepatic cells can increase the  
165 inflammatory response in recipient macrophage cells, we treated phorbol 12-myristate-13-  
166 acetate (PMA)- differentiated U937 macrophages with EVs isolated from cholesterol-lipid  
167 concentrate treated Huh7 cell. There, similar to what was noted in murine liver, addition of  
168 lipid induced hepatocyte-derived EVs elevated pro-inflammatory cytokine mRNA levels in  
169 human macrophage cells (Figure 2C).

170 To determine the contribution of hepatic cell derived EVs in the induction of the  
171 inflammatory phenotype, mouse primary hepatocyte cells were first treated with cholesterol-  
172 lipid concentrate for 4 hours. EVs from the cell culture supernatant were then added to  
173 murine primary macrophages (Kupffer cells). Increased mRNA levels of the pro-inflammatory  
174 cytokines TNF $\alpha$ , IL-6 and IL-1 $\beta$  were observed in recipient Kupffer cells upon treatment with  
175 EVs derived from lipid treated primary hepatocytes (Figure 2D). RT-qPCR assays detected  
176 increased levels of internalized miR-122 in the recipient macrophage cells as compared to  
177 control (Figure 2E). However levels of internalized miR-16, another miRNA known to  
178 increase in circulation in high-lipid condition (Tan et al., 2014) remained unaffected (Figure  
179 2E). To determine the miR-122 dependence of this phenomenon, we isolated EVs from  
180 cholesterol-lipid treated Hepa1-6 cells expressing miR-122 and added them to RAW 264.7  
181 cells. Like in primary macrophage cells, RAW264.7 cells receiving the EVs from miR-122



182 transfected and cholesterol treated Hepa 1-6 cells also showed increased expression of pro-  
183 inflammatory cytokines (Figure 2F). In the subsequent experiment, to confirm the  
184 immunostimulatory role of miR-122 transferred from lipid challenged hepatic cells, receiving  
185 RAW264.7 cells were transfected with anti-miR-122 oligos. Anti-miR-122 transfected cells  
186 showed marked decrease in various proinflammatory cytokine mRNAs like TNF- $\alpha$ , IL-1 $\beta$  and  
187 IL-6 expression even after treatment with cholesterol-lipid treated Hepa1-6 EVs (Figure 2G).  
188 These results strongly suggest the pro-inflammatory nature of the miR-122 exported from  
189 lipid loaded hepatic cells. The extracellular miR-122, taken up by receiving macrophages,  
190 enhances the expression of proinflammatory cytokines and thereby ensures a more  
191 activated state of inflammation in the recipient cells.

192 To make a strong correlation of EV-derived miR-122 and inflammatory response, we  
193 expressed miR-122 from a doxycycline (DOX) inducible expression vector in naive  
194 RAW264.7 cells and checked cytokine mRNA levels over time when cells were incubated  
195 with DOX. The induction of miR-122 resulted in an accumulation of mature miR-122 over  
196 time upon induction with DOX. The increase in cellular miR-122 levels was found to correlate  
197 with the cytokine mRNAs' expression increase (Figure 2 H and I). Interestingly after a  
198 threshold of expression, happening at 24h of miR-122 induction, effectiveness of miR-122  
199 for cytokine induction gets impaired possibly due to jeopardized miRNP balance happening  
200 for other important miRNAs present there.

201 Do the EVs released by hepatic cells enter and affect the cytokine expression in tissue  
202 resident macrophages? We isolated EVs packed with miR-122 from the culture supernatant  
203 of HePa1-6 cells expressing miR-122. The EVs were injected into normal BALB/c mice  
204 (adult, 8-10 weeks) mice through tail-vein and hepatic non-parenchymal cells were isolated  
205 and analyzed for expression of different cytokines (Supplementary Figure S1A). Compared  
206 to PBS injected groups, mice injected with miR-122 containing EVs showed an increase in  
207 miR-122 levels in isolated hepatic non parenchymal cells, along with an elevation in

208 inflammatory cytokines' expression (Supplementary Figure S1B-C). The circulatory miR-122  
209 level in miR-122 EV injected mice also showed an elevation with no corresponding change  
210 in serum miR-16 level (Supplementary Figure S1D). These data suggest miR-122 containing  
211 EV dependent inflammatory response in murine liver.

### 212 **Blocking of MMP2 affects miRNA cargo transfer between human cells**

213 How do EVs move within the matrix of a tissue? In the liver, the extracellular matrix is rigid  
214 and composed of high levels of collagen. We expect, presence of specific proteases on the  
215 surface of EV may do the job to degrade the matrix and matrix metalloproteases (MMPs) are  
216 the best candidate for doing that. We were exploring the effect of different inhibitors and  
217 factors specific siRNAs against MMPs to score their effect on EV-mediated miRNA transfer  
218 in human cells in a microscopy based assay. In this assay the recipient HeLa cells were  
219 grown on coverslip in a 24 well cell culture format with the insert. The insert separated the  
220 upper compartment that was used for layering of Matrigel<sup>R</sup>. Isolated EVs from human  
221 hepatoma cell Huh7 transfected with Cy3-labeled miR-122 were used to study the transfer of  
222 Cy3 labeled miR-122 to recipient HeLa cells. The isolated EVs were added in the upper  
223 chamber which separated the EVs from target cells present in the lower chamber by a  
224 Matrigel<sup>R</sup> layer. The transferred Cy3 labelled miRNAs were visualized by subjecting the  
225 recipient cell co-stained for tubulin to confocal microscopy imaging (Figure 3A). The  
226 inhibitors were applied in the upper chamber while SiRNA against specific proteins were  
227 used for co-transfection along with Cy3-miR-122 in donor Huh7 cells used for collecting EVs.  
228 The EVs used in the experiment were analyzed by Nanoparticle tracking analyzer (Figure  
229 3B). We documented defective Cy3-miR-122 transfer happening in cells treated with  
230 ARP101 as an inhibitor of MMP2 (Jo et al, 2011). Similar results were also observed with  
231 EVs isolated from MMP2 deficient Huh7 donor cells (Figure 3C and E). Interestingly transfer  
232 of GFP-tagged CD63 positive EVs was also found to be impaired by ARP101 and siMMP2  
233 when EVs were isolated from Huh7 cells expressing CD63-GFP (Figure 3D and F).

## 234 **Functional transfer of miRNA from hepatic cells requires MMP2**

235 What function does MMP2 have on EV-mediated cargo transfer between hepatic cells? To  
236 explore the exact role of MMP2 in miRNA transfer, we incubated miR-122 containing EVs  
237 derived either from naive or pmir-122 transfected Huh7 cells with recipient HepG2 cells  
238 grown in Matrigel<sup>R</sup>. We documented a transfer of miRNA into HepG2 cells that otherwise  
239 don't express miR-122. Further, we noticed blocking of this transfer of miRNA when  
240 incubated with ARP101, the MMP2 inhibitor. Treatment of donor Huh7 cells with anti-miR-  
241 122 blocks the transfer of functional miR-122 to recipient cells (Figure 4A). Similar level of  
242 miR-122 transfer from donor HeLa cells, ectopically expressing miR-122, to HepG2 has  
243 been documented and the MMP2 inhibitor blocked the transfer of miR-122 (Figure 4B). Do  
244 the transferred miRNA become functionally active in the recipient cells? We used miR-122  
245 reporter mRNA to test the functional transfer of miR-122 in recipient cells. The transferred  
246 miR-122 could repress the RL-reporter having one perfect miR-122 sites in HepG2 recipient  
247 cells and a fold repression of the reporter has been scored against the RL reporter without  
248 miRNA binding sites (Figure 4C-D)(Basu & Bhattacharyya, 2014). Blocking of MMP2  
249 stopped the miR-122 activity transfer to recipient HepG2 cells both from Huh7 and HeLa  
250 donor cells (Figure 4E and F). Interestingly, when EVs isolated from Huh7 cells expressing  
251 miR-122 were incubated with Huh7 cells we could see a drop in cellular miR-122 content.  
252 This may be explained by a reduced self-transfer of miR-122 to the donor cell that itself  
253 gets reduced in presence of MMP2 inhibitor ARP101 (Figure 4G). The results described  
254 here point out to an important role of MMP2 in transfer of functional cargo miRNA in  
255 mammalian cells and thus is an essential component of miRNA activity regulation in a tissue.

## 256 **MMP2 present on liver cell derived EVs and its association with EVs is dependent on** 257 **MMP14**

258 Presence of MMP2 with the exosomes isolated from human cells has been reported before  
259 where the MMP2 was found to promote the effect of exosomes on target cells (Tang et al,

260 2019). We have found presence of MMP2 in EVs isolated from liver and non-liver cells. We  
261 detected mature MMP2 in the EVs isolated from control Huh7 cells or cells expressing  
262 excess miR-122 (pmiR-122 transfected) and from Huh7 cells inactivated for miR-122 by anti-  
263 miR-122 treatment. In all cases we detected MMP2 in Gelatin zymography and by western  
264 blot (Figure 5A and B). We also detected MMP2 by western blot in EVs derived from non-  
265 hepatic cell HeLa (Figure 5B left panel). The mature form of the MMP2 was not detected in  
266 Huh7 and HeLa cells but mature MMP2 was predominantly found in the EVs. The EV  
267 associated MMP2 was found to be sensitive to Proteinase K treatment and no MMP2 was  
268 detected with EVs after proteinase K treatment (Figure 5C). These results suggest the  
269 presence of MMP2 on the outer side of the EVs. MMP14 is known to retain the MMP2 with  
270 cell and EV's membrane (Han et al, 2015). To explore the retention mechanism of MMP2  
271 with EVs, we inactivated MMP14 to check the presence of MMP2 associated with EVs.  
272 Depletion of MMP14 in Huh7 cells followed by isolation of EVs and western blotting for  
273 MMP2 showed a decrease in MMP2 levels in EVs isolated from MMP14 compromised Huh7  
274 cells (Figure 5D). Our data suggest presence of MMP2 on the outer side of the EV  
275 membrane is dependent on MMP14 and the MMP2 is required for intercellular EV-transfer  
276 across the cell boundaries.

### 277 **MMP2 facilitate EV movement across extracellular matrix and also enhance EV-entry** 278 **in mammalian cells**

279 Why MMP2 is required for the EV-cargo delivery? It is possible that MMP2 presence on EV  
280 enable them to migrate through the extracellular matrix by degrading the extracellular mesh  
281 made up of collagen and ensure a faster movement of the EV across the matrix. To test that,  
282 we used a collagen matrix and in a "EV-Movement" monitoring assay, we measured the EV  
283 movement across the matrix in presence and absence of ARP101 as MMP2 inhibitor or in  
284 presence of rMMP2. In control and rMMP2 presence we documented movement of EV front  
285 in collagen matrix measured by the rate of movement in unit time. While we documented no

286 specific movement of EV front in presence of ARP101, confirming the importance of MMP2  
287 in EV-movement across extracellular space (Supplementary Figure S2A-C). Does MMP2  
288 also help in the internalization of EV? We did the EV-uptake experiment done in 2D cell  
289 culture without a Matrigel<sup>R</sup> matrix. We noted the MMP2 dependent uptake of CD63-GFP  
290 positive EV entry in HeLa cells as the entry of CD63-GFP positive vesicles get retarded in  
291 presence of MMP2 inhibitor ARP101 (Supplementary Figure S2D-E). This data suggests a  
292 possible role of MMP2 in ensuring the movement of EVs across the matrix and its uptake in  
293 hepatic cells.

### 294 **Trafficking of miRNA containing EVs in mouse liver from hepatic cells to macrophage** 295 **require MMP2**

296 How does MMP2 affect the functional transfer of miRNA via EVs in a physiological context?  
297 miR-122 is a hepatocyte derived proinflammatory miRNA that when transferred to naive  
298 macrophage cells can activate them. To score the effect of MMP2 inhibition on transfer of  
299 hepatic EVs to resident macrophages, we adopted similar experimental set up as described  
300 in Figure 3A where the recipient macrophage cells were grown in the bottom chamber of a  
301 12 well multi-well plate with insert and hepatocyte derived EVs were added on the upper  
302 chamber layered on top a Matrigel<sup>R</sup> layer along with DMSO or ARP101 as MMP2 inhibitor.  
303 We scored the transfer of miR-122 to recipient Raw264.7 monocytes and measured the  
304 proinflammatory cytokine levels there (Figure 6A). We have documented upregulation of  
305 proinflammatory cytokines in cells where miR-122 were also getting transferred.  
306 Interestingly, blocking of miR-122 transfer by MMP2 inhibitor also affects the  
307 proinflammatory cytokine expression there (Figure 6A-B). To make a direct correlation  
308 between MMP2 and proinflammatory response in recipient RAW264.7 cells, we treated the  
309 EVs with rMMP2 and documented a positive influence of rMMP2 on proinflammatory  
310 response induced by hepatic EVs in RAW264.7 cells. (Figure 6B).

311 To score the *in vivo* effect of the MMP2 inhibition in induction of inflammatory response by  
312 hepatic EVs with miR-122, we expressed miR-122 in Hepa1-6 cells and isolated the EVs.  
313 The EVs were injected through tail-vein injection in recipient mice alone or with MMP2  
314 inhibitor ARP101. We documented reduced levels of pro-inflammatory cytokine expression  
315 and miR-122 transfer in non-parenchymal hepatic cell population in animals livers injected  
316 with ARP101 (Figure 6C-D). Our data suggests the importance of MMP2 for intra-tissue  
317 miRNA transfer in mouse liver.

318

## 319 Discussion

319

320 In the work described above, we have identified how the matrix metalloproteinase MMP2 by  
321 facilitating the movement of EVs through the extracellular matrix affects the functional  
322 miRNA transfer in the hepatic context and plays a role in liver-specific miRNA-mediated  
323 inflammation. miRNA transfer between similar or different types of cell in a tissue causes  
324 miRNA homeostasis but how the miRNA expression levels are controlled by the factors that  
325 affect the transfer process per se are unknown.

325

326 Extracellular vesicles (EVs) help in cell to cell communication and, like hormones,  
327 can have an autocrine, paracrine or endocrine effect (Becker et al, 2016). miRNAs packaged  
328 in EVs are speculated to fine tune the gene expression profile in neighbouring cells and  
329 tissues and thus, could facilitate metabolic and functional homeostasis in respective tissues  
330 (Chevillet et al, 2014; Lotvall & Valadi, 2007). In the current work, miR-122 enriched EVs  
331 secreted from lipid loaded Huh7 cells have been shown to elicit a pro-inflammatory response  
332 in recipient macrophages. Is there a reciprocal effect of secreted pro-inflammatory cytokines  
333 on Huh7 cells? The released cytokines may bind to receptors on Huh7 cells and affect the  
334 transcription flux of HuR other factors that mediate the extracellular export pathway  
335 (Mukherjee et al, 2016). Possibility of the existence of such a feedback loop could help to

336 curb the pro-inflammatory response in macrophages and could also, fine tune the miRNA  
337 profile in Huh7 cells and, thus could help in the attainment of tissue level homeostasis in  
338 gene expression. Deciphering the mechanism of such a feedback loop can be looked into in  
339 future studies. The propagation of inflammatory miR-122 as part of EVs in the blood of high  
340 fat diet fed mice raises the possibility of the miRNA being taken up by far located tissue  
341 macrophage in other organs where it may play a role in ectopic activation of the immune  
342 cells across the tissue boundary and thus, contribute to a chronic systemic inflammatory  
343 response in mice exposed to high-fat diet.

344 miRNA transfer can be controlled at three different steps; the packing and export of  
345 the miRNAs via EVs, the movement of EVs through the extracellular matrix and  
346 internalization and release of content of EVs in the recipient cells. Exploration of all three  
347 steps is largely limited in identification of the few factors individually controlling these steps.  
348 HuR is one such protein that has been identified as the facilitator of export of specific subset  
349 of miRNAs including miR-122 from hepatic cells to ensure its export in stress conditions  
350 (Mukherjee et al, 2016). This protects the hepatic cells from stress. The effect of stress on  
351 MMP2 has been known and it also seems to have limited effect on MMP2 present on the  
352 EVs released by the hepatic cells under stress condition (data not shown). From the data  
353 described here, MMP2 expression also seems to remain unaffected in Huh7 cells at protein  
354 level after expression of excess miR-122. miR-122 after getting into hepatic cells also  
355 decreases factors preventing its expression such as hepatic Insulin like growth factor 1 to  
356 ensure robust miR-122 expression (Basu & Bhattacharyya, 2014).

357 miRNAs, as epigenetic signals should exchange between neighbouring cells in a  
358 functional form and to ensure that they are transferred as single stranded form and getting  
359 incorporated into recipient cell Ago2 protein (unpublished data) and plays an important role  
360 in controlling the expression of target mRNA in both donor and recipient cells. To ensure the  
361 effective transfer of miRNAs, the movement of EVs through the matrix is an important factor

362 and several biochemical and physical properties of the matrix should have contributed to  
363 controlling the speed of the movement. The collagen network and extracellular proteases  
364 must work in a reciprocal manner to ensure the movement. The concentration and  
365 maturation of MMPs should be the key aspects that should determine the EVs movement. In  
366 tumour microenvironment, the multidimensional movement of cancer cell derived EVs  
367 contributes in the establishment of cancer cell niche by affecting the gene expression of non-  
368 cancerous and immune cells present in the tumour. Variable expression of MMPs by cancer  
369 cells are known to be essential for niche creation. We propose the MMP-mediated facilitation  
370 of the EV's movement may thus contribute to cancer progression by ensuring a rapid  
371 movement of EVs in 3D. Blocking of EV-transport by targeting MMPs would thus be an  
372 effective way of controlling miRNA transport in mammalian cells and may be an useful tool to  
373 curtail cancer tumour growth.

## 374 **Experimental Procedures**

### 375 **Cell Culture, Reagents and Antibodies**

376 Human HCC cell lines (Huh7, HepG2) and Human HeLa were cultured in Dulbecco's  
377 modified Eagle's medium (DMEM; Gibco-BRL) supplemented with 10% fetal bovine serum  
378 (FBS; GIBCO-BRL) and Penicillin Streptomycin (1X) antibiotics (GIBCO). RAW264.7 were  
379 cultured in RPMI (Gibco-BRL) supplemented with 10% fetal bovine serum (FBS; GIBCO-  
380 BRL) and Penicillin Streptomycin (1X) antibiotics (GIBCO).

381 MMP2 inhibitor, ARP101 was purchased from Sigma-Aldrich; recombinant MMP2 was  
382 purchased from Calbiochem. DMSO was obtained from Fisher Scientific.

383 Human Alix (Santa Cruz), CD63 (BD Pharmingen), MMP2 (Cell Signaling Technologies),  
384 Actin (Sigma-Aldrich) and secondary mouse and rabbit antibodies (Invitrogen) were  
385 purchased.

### 386 **Plasmid constructs, Cell transfections and Luciferase assay**

387



388 The RL reporters (Renilla luciferase) were previously described (Pillai et al., 2005).

389 siControl and siMMP2 were used for transfection at 100 pmoles per well of a confluent six-  
390 well plate. miR-122 and anti-miR-122 were purchased from Ambion and was used at 100  
391 pmoles to transfect cells per well of a six-well plate. Cells were differentially transfected  
392 microscopy using CD63-GFP, Tubulin-GFP and cy3-miR122 plasmids. For transfections 1µg  
393 of the plasmids was used for transfecting  $10^6$  cells in a 10cm<sup>2</sup> well. All transfections were  
394 performed using Lipofectamine 2000 (Invitrogen) following manufacturer's instructions.

395 For luciferase assays  $10^6$  cells in a 10 cm<sup>2</sup> well were transfected with either RL-con or RL-  
396 per-miR-122 plasmids in parallel sets. To detect fold repression in HepG2,  $10^6$  cells in a 10  
397 cm<sup>2</sup> well were transfected with 150 ng of each of the plasmids. Normalisation was done with  
398 a Firefly (FF) luciferase construct which was co-transfected along with the RL constructs  
399 (1µg for  $1 \times 10^6$  cells) after 24 h of transfection, cells were split After that cells were lysed  
400 with 1 X Passive Lysis Buffer (Promega). Renilla (RL) and Firefly (FL) activities were  
401 measured using a Dual-Luciferase Assay Kit (Promega) following the suppliers protocol on a  
402 VICTOR X3 Plate Reader with injectors (Perkin Elmer). Mean Fold Repression was  
403 calculated by dividing the FF normalized RL-Con value with that of FF normalized RL-per-  
404 miR-122 value. Relative fold repression was calculated by taking the control mean fold  
405 repression as 1. All luciferase assays used in this study have been done in triplicate. All  
406 experiments were performed minimum three times before the SD values were calculated.

#### 407 **Cholesterol and Palmitic Acid treatment:**

408 MβCD conjugated cholesterol conjugate obtained from GIBCO (#12531-018) was added  
409 from a 250X stock to Huh7 cells in culture at a final concentration of 5X for a period of 4  
410 hours. Cholesterol treatments were done to Huh7 cells in fresh growth media at 70-80%  
411 confluency. Unless otherwise mentioned, cholesterol treatment was done at a final  
412 concentration of 5x for 4 hours.

#### 413 **Animal experiments**

414 All animal experiments were approved by the Institutional Animal Ethics Committee  
415 (approved by CPCSEA, Ministry of Environment & Forest, and Government of India). 8-10  
416 weeks old male (20-24g) C57BL/6 mice were housed under controlled conditions  
417 (temperature  $23 \pm 2^\circ\text{C}$ , 12 hour/12-hour light/dark cycle) in individually ventilated cages. Mice  
418 were randomly divided into two groups and fed either standard chow diet or methionine and  
419 choline deficient diet MCD (MP Biomedicals; #0296043910) up to four weeks.

420 C57BL/6 male mice of 8-10 weeks age were divided in two groups for normal chow and high  
421 fat diet (HFD) containing 45% fat and 5.81 kcal/gm diet energy content (MP Biomedicals; #  
422 960192). Animals were fed with HFD for 4 weeks.

423 For isolation of RNA from tissues, TRIzol® (Invitrogen) reagent was used. For  
424 analysis of EV-associated RNA, serum fraction of blood was used. Relative levels of miRNA  
425 and mRNA in serum and tissues were quantified by qRT-PCR.

426 For histological analysis, tissues were fixed in 10% formaldehyde in PBS, embedded  
427 in paraffin, sectioned at 10  $\mu\text{m}$ , and stained with hematoxylin and eosin (H&E) following  
428 standard staining protocol.

429 For exosome injection experiments, Hepa1-6 cells were transfected with miR-122  
430 expressing plasmids ( $6\mu\text{g}/6 \times 10^6$  cells). Approximately  $1 \times 10^9$  exosomes (measured by  
431 Nanoparticle Tracking Analysis- Nanosight Malvern U.K.) isolated from transfected Hepa1-6  
432 cells ( $\sim 1 \times 10^7$  cells) were suspended in 1x PBS (passed through 0.22 $\mu\text{m}$  filter units in 100  
433  $\mu\text{l}$ ) and injected into the tail vein of BALB/c mice (adult, 8-10 weeks). Control mice were  
434 injected with equal volume of 1x PBS (passed through 0.22 $\mu\text{m}$  filter units). Experiment was  
435 performed with 5 mice in each group (control injected and exosome injected). Injections  
436 were repeated every alternate day for three days and mice sacrificed the next day after the  
437 third injection. Animals were anaesthetized and livers were slowly perfused initially with the  
438 HBSS and then with 0.05% collagenase buffer via the portal vein. Livers were then excised,

439 minced and filtered through a 70 µm cell strainer. The resultant single cell suspension was  
440 centrifuged at 50Xg for 5 minutes to precipitate and remove the hepatocytes. The  
441 supernatant was then collected and centrifuged at 250g for 15 minutes. The pellet was  
442 resuspended in RBC lysis buffer and kept in ice for 10 minutes. The resultant cell  
443 suspension was again centrifuged at 250xg for 15 minutes and pellet obtained was lysed  
444 with Trizol reagent. For detection of serum miRNA levels, serum fraction of blood was used.  
445 Blood samples were collected by cardiac puncture and allowed to clot. Serum was  
446 separated by centrifugation and frozen at -80°C.

### 447 **Liver macrophage sorting and analysis by flow cytometry (FACS)**

448 Animals were anaesthetized and livers were slowly perfused initially with the HBSS and then  
449 with 0.05% collagenase buffer via the portal vein. Livers were then excised, minced and  
450 filtered through a 70µm cell strainer. The resultant single cell suspension was centrifuged at  
451 250 g for 5 minutes to obtain non parenchymal cells and on the basis of surface staining with  
452 anti-F4/80 (FITC), anti-CD11b (APC) (eBioscience) antibodies, three types of liver  
453 macrophages were sorted by FACS (Beckman Coulter).CD11b+, F4/80+ and Cd11b+F4/80+  
454 cells were sorted. Unstained cells were used for setting compensation and gates.

### 455 **Primary Hepatocyte Isolation**

456 Animals were obtained from the animal house of the institute and all experiments were  
457 performed according to the guidelines set by Institutional Animal Ethics committee following  
458 the Govt. of India regulations. Mouse primary hepatocytes were isolated using the  
459 hepatocyte product line from Gibco Invitrogen Corporation. Adult BALB/c mice (4-6 weeks)  
460 were anaesthetized and the portal vein was cannulated using a 25G butterfly cannula and  
461 an incision was made in the inferior vena cava. The liver was perfused with 350 mL of warm  
462 (37°C) Liver Perfusion Medium (Cat. No. 17701) at a rate of 35 mL/minute with the perfusate  
463 exiting through the severed vena cava. This was followed by a Collagenase-Dispase

464 digestion with Liver Digest Medium (Cat no. 17703) at a rate of 35 mL/minute. The liver was  
465 then aseptically transferred to the tissue culture hood on ice in Hepatocyte Wash Medium  
466 (cat no. 17704). Using blunt forceps the digested liver was torn open to release the  
467 hepatocytes. Cell clumps were dissociated by gently pipetting the solution up and down  
468 using a 25ml pipette. The solution was then filtered through 100  $\mu$ M nylon caps atop 50 ml  
469 conical tubes. The cell suspension was then centrifuged at 50 x g for 3 min. The pellet was  
470 gently resuspended in 10 ml of Wash Medium using 25 ml pipette and the centrifugation  
471 repeated.

472 Cells were finally resuspended in Hepatocyte Wash Medium with 10% FCS and plated at  
473  $1 \times 10^7$  cells /ml. Cells were plated in tissue culture treated collagen (Gibco Cat. No. A10483-  
474 01) coated plates at 12.5  $\mu$ g/cm<sup>2</sup>. Unattached cells are poured off 4h after plating and  
475 medium was replaced with Hepatozyme-SFM (Cat no. 17705) with glutamine and 1%  
476 Pen/Strep. Cholesterol and BSA-Palmitate was added the next day in Hepatozyme-SFM.

477 For Kuppfer cell isolation, supernatant obtained from the first centrifugation (at 50x g for 3  
478 minutes) after filtering through the 100  $\mu$ m cell strainer was further centrifuged at 250xg for 5  
479 min. The cell pellet was washed, resuspended in DMEM with 10% FBS, seeded onto tissue  
480 culture plates, and allowed to adhere for 16 h. Nonadherent cells were removed by several  
481 washes with PBS; >80% adherent cells were found to be positive for F4/80, a well-  
482 established KC marker.

### 483 **Exosome Isolation**

484 For exosome isolation cells were grown in media made from exosome depleted FCS which  
485 were prepared by ultracentrifugation of the FCS used at 110,000xg for 5 h. The supernatant  
486 CM from one 90 cm<sup>2</sup> plates, having  $1 \times 10^6$  donor cells (Huh7) was taken. The CMs were  
487 centrifuged first at 300xg for 10 min, then at 2000xg for 15 min followed by centrifugation at  
488 10,000xg for 30 min. All centrifugations were done at 4°C. The CM was then filtered through  
489 a 0.22  $\mu$ m filter unit. This was then centrifuged at 100,000xg for 90 min at 4°C. After

490 centrifugation, the supernatant was discarded. The pellet was resuspended in media and  
491 added back to recipient cells (HepG2) in a 24-well format such that  $1 \times 10^5$  recipient cells  
492 received the exosomes from  $1 \times 10^6$  donor cells. For CM based assays the same ratio was  
493 followed with CM from  $10^6$  cells being added to  $2 \times 10^5$  cells. For the isolation of miR-122,  
494 anti-miR-122, Huh7, HeLa and HepG2 carrying exosomes,  $1 \times 10^6$  cells were transfected  
495 and 24 h after transfection, the cells were reseeded onto a 90 cm<sup>2</sup> plate. Cells were grown  
496 for 48–72 h and exosomes isolated from the CM of these cells. For the exosomal protein  
497 isolation experiment, the CMs were centrifuged first at 300 x g for 10 mins, then at 2000 x g  
498 for 15 min followed by centrifugation at 10,000 x g for 30 mins. All centrifugations were done  
499 at 4°C. The CM was then filtered through a 0.22 µm filter unit and was loaded on a sucrose  
500 cushion (1 M sucrose and 10 mM Tris–HCl pH 7.5). This was ultracentrifuged at 120,000 x g  
501 for 90 mins at 4°C. The medium above the sucrose cushion was discarded leaving behind a  
502 narrow layer of medium with the exosomes at the interface. 1XPBS was added and the  
503 separated exosomes were washed at 4°C for 90 mins at 100,000 x g. The pellet was  
504 resuspended in 200µl of 1X SDS Buffer, which was used for western analysis for exosome  
505 markers.

### 506 **Gelatin Zymography and invitro EV Movement assay**

507 Human HCC cells (Huh7 and HepG2) and a non hepatic cell line HeLa were transfected with  
508 miR122 expressing plasmid PJC148 and anti-miR122 oligonucleotides, media was changed  
509 after 6 hours and incubated for o/n at 37°C humidified incubator. Cells were split to 90mm  
510 culture dishes containing DMEM with 2% Exo depleted FCS and kept for 24 hrs at incubator.  
511 Exosomes were isolated and EDTA free protease inhibitor cocktail containing lysis buffer  
512 was added to isolated exosomes and 8% gelatin containing SDS-PAGE gel was run at 60v  
513 for 3 hrs. After the completion of the run gels were washed for 1hr in 2.5x Triton X and then  
514 gels were incubated in calcium assay buffer (40 mM Tris-HCl, pH 7.4, 0.2 M NaCl, 10 mM  
515 CaCl<sub>2</sub>) for o/n at 37°C incubator. After incubation in buffer, gels were stained with 0.1%  
516

517 coomasie blue and then destaining was followed. The zones of gelatinolytic activities  
518 appeared as negative staining. Images of zymographic bands were performed using an UVP  
519 Biolumager 600 system equipped with VisionWorks Life Science software (UVP) V6.80.

520 For the diffusion rate measurement assay, Huh7 released EVs were pretreated with rMMP2  
521 or ARP101. EVs were isolated from culture supernatant of Huh7 cells ( $1 \times 10^7$  Cells) and  
522 were then spotted on a well formed in the middle of a 35mm Petri dish layered with 2mm  
523 thick gelatine matrix. After 30 minutes the reaction was stopped by placing the gel for  
524 staining with Brilliant Blue to visualize the diffusion front of the EVs through the matrix. The  
525 representative plate photographs were taken and distance travelled by the MMP2 containing  
526 EVs were measured from the center by visualizing and measuring the distance of the front  
527 visible in individual cases.

528

### 529 **Western blotting**

530

531 Cells were lysed in 1X Passive Lysis Buffer (PLB) (Promega) and quantified using Bradford  
532 reagent (Thermo Scientific). Cell number equivalent amount of the sample is then diluted in  
533 5X Sample Loading Buffer (312.5 mM Tris-HCl, pH 6.8, 10% SDS, 50% glycerol, 250 mM  
534 DTT, 0.5% bromophenol blue) and heated for 10 mins at 95°C. Usually  $1/5^{\text{th}}$  of the total  
535 amount from a  $4\text{cm}^2$  well was loaded for both the control and experimental samples.  
536 Following SDS-polyacrylamide gel electrophoresis of the extracts, proteins were transferred  
537 to PVDF nylon membranes. Membranes were blocked in TBS (Tris-buffered saline)  
538 containing 0.1% Tween-20 and 3% BSA. Primary antibodies were added in 3% BSA for a  
539 minimum 16 hr at 4°C. Following overnight incubation with antibody, the membranes were  
540 washed at room temperature thrice for 5 min with TBS containing 0.1% Tween-20. Washed  
541 membranes were incubated at room temperature for 1 hr with secondary antibodies  
542 conjugated with horseradish peroxidase (1:8000 dilutions). Excess antibodies were washed  
543 three times with TBS-Tween-20 at room temperature. Antigen-antibody complexes were  
detected with West Pico Chemi luminescent substrate using standard manufactures protocol

544 (Perkin Elmer). Imaging of all western blots was performed using an UVP Biolumager 600  
545 system equipped with VisionWorks Life Science software (UVP) V6.80.

### 546 **Fluorescence Microscopy**

547 Gelatin coated cover slips are added onto a 24 well plate. Recipient HeLa cells were seeded  
548 onto those cover slips such that they become 40% confluent after 24 hours. Exosomes from  
549 donor cells were added to 24-well inserts coated with 3mg/ml Matrigel and incubated for 24-  
550 48hrs. The recipient cells were washed with 1X PBS and fixed using 4% paraformaldehyde  
551 in 1X PBS for 30 mins in the dark at room temperature. Cover slips were then washed thrice  
552 with 1X PBS. Primary antibody incubation was done in 1XPBS with 1% BSA at 4°C overnight  
553 in a humid chamber. The anti-Tubulin antibody was used at a dilution of 1:100. Secondary  
554 antibody incubation was done in 1XPBS with 1% BSA for 1h at room temperature.  
555 Secondary anti-mouse antibodies labeled either with Alexa Fluor® 488 secondary antibodies  
556 (green) or Alexa Fluor® 568 (Red) (Invitrogen) were used at 1:500 dilutions. The cells were  
557 subsequently washed thrice with 1X PBS. Coverslips were then mounted with Vectashield  
558 containing DAPI and observed under a fluorescence microscope. Images were captured with  
559 a Zeiss LSM800 microscope. All post capture analysis and processing were done using  
560 Imaris 7 (BitPlane) software.

### 561 **Post Capture Image analysis**

562 All western blots were processed with Adobe Photoshop CS4 for all linear adjustments and  
563 cropping. All images captured on Zeiss LSM800 microscope were analyzed and processed  
564 with Imaris 7 (Bitplane) software.

### 565 **Quantitative estimation of mRNA and miRNA levels**

566 RNA was extracted by using the TRIzol reagent according to the manufacturer's protocol  
567 (Invitrogen). Real time analyses by two-step RT-qPCR was performed for quantification of  
568 miRNA and mRNA levels. All mRNA RT-qPCRs were performed on a 7500 REAL TIME  
569 PCR SYSTEM (Applied Biosystems). mRNA real time quantification was generally  
570

571 performed in a two step format using Eurogentec Reverse Transcriptase Core Kit and MESA  
572 GREEN qPCR Master Mix Plus for SYBR Assay with Low Rox kit from Eurogentec following  
573 the suppliers' protocols. Reactions were performed with 50ng of cellular RNA. The RT  
574 reaction condition was 25°C, 10 min; 48°C, 30min; 95°C, 5 min. The PCR condition was  
575 95°C, 5 min; 95°C, 15 sec; 60°C, 1 min; for 40 cycles. The comparative  $C_t$  method which  
576 typically included normalization by 18S rRNA levels for each sample was used for relative  
577 quantification. Details of mRNA gene specific primers are given below.

578 Quantification of miRNA levels was done using Applied Biosystem TaqMan® chemistry  
579 based miRNA assay system. All mRNA RT-qPCRs were performed on Biorad CFX96 Real  
580 Time System. Assays were performed with 25 ng of cellular RNA, using specific primers for  
581 human miR-122, miR-16 and miR-21 (assay ID 000445, 000391, 000397 respectively). U6  
582 snRNA (assay ID 001973) was used as an endogenous control. One third of the reverse  
583 transcription mix was subjected to PCR amplification with TaqMan® Universal PCR Master  
584 Mix No AmpErase (Applied Biosystems) and the respective TaqMan® reagents for target  
585 miRNA. The RT reaction condition was: 16°C, 30 min; 42°C, 30 min; 85°C, 5 min; 4°C, □.  
586 The PCR condition was: 95°C, 5 min; 95°C, 15 sec; 60°C, 1 min; for 40 cycles. For detection  
587 of miRNAs in exosomal fractions, 100ng of RNA was used for reverse transcription.

588 Samples were analyzed in triplicates. The concentrations of intra cellular miRNAs and  
589 mRNAs were calculated based on their normalized  $C_t$  values. The  $\Delta\Delta C_t$  method for relative  
590 quantitation (RQ) of gene expression was used and relative quantification was done using  
591 the equation  $2^{-\Delta\Delta C_t}$  (as per 'Guide to Performing Relative Quantitation of Gene Expression  
592 Using Real-Time Quantitative PCR' obtained from the Applied Biosystems website  
593 ([http://www3.appliedbiosystems.com/cms/groups/mcb\\_support/documents/generaldocument](http://www3.appliedbiosystems.com/cms/groups/mcb_support/documents/generaldocument/s/cms_042380.pdf)  
594 [s/cms\\_042380.pdf](http://www3.appliedbiosystems.com/cms/groups/mcb_support/documents/generaldocument/s/cms_042380.pdf)).

#### 595 mRNA RT-qPCR Primer Sequences



596 Mouse TNF $\alpha$ : Forward: 5'-GTCTCAGCCTCTTCTCATTCC-3'; Mouse TNF $\alpha$ : Reverse: 5'-  
597 TCCACTTGGTGGTTTGCTACG-3'; Mouse IL6: Forward: 5'-AGGATACCACTCCCAACAGA-  
598 3'; Mouse IL6: Reverse: 5'-GTA CTCCAGAAGACCAGAGGA-3'; Mouse IL1 $\beta$ : Forward: 5'-  
599 GACCTTCCAGGATGAGGACAT-3'; Mouse IL1 $\beta$ : Reverse: 5'-  
600 CCTTGTACAAAGCTCATGGAG-3'; 18S rRNA: Forward: 5'-TGACTCTAGATAACCTCGGG-  
601 3'; 18s rRNA: Reverse: 5'-GACTCATTCCAATTACAGGG-3'.

### 602 **Statistical Analysis**

603 All graphs and statistical analyses were generated in Graph-Pad Prism 5.00 (GraphPad, San  
604 Diego, CA, USA). Nonparametric unpaired t-test and paired t test were used for analysis,  
605 and P values were determined. Error bars indicate mean  $\pm$ SEM.

### 607 **Acknowledgements**

608 We thank Witold Filipowicz and Gunter Meister for different constructs used in this study. We  
609 thank the Funding body, Dept. of Science and Technology (DST), Govt. of India and Council  
610 for Scientific and Industrial Research (CSIR), and University Grant Commission (UGC) for the  
611 fellowship to DB, SB, S.C and MA. SB and D.D. also acknowledges the support from  
612 Department of Biotechnology, Govt of India and Dept. of Science and Technology (DST),  
613 Govt. of India for their fellowship support. SNB was supported by SwarnaJayanti Fellowship  
614 and a High Risk High Reward Grant from DST.

### 616 **Author Contributions**

617 S.N.B. conceived the idea, designed the experiments, analyzed the data and wrote the  
618 manuscript. S.B., A.D., S.S and P.C. have contributed in design and planning the  
619 experiments. A.D. S.B.,S.C., D.D., and M.A. performed the experiments. S.B. and D.B also  
620 wrote the manuscript with S.N.B. and analyzed the data.

621

622 **Conflict of Interest**

623 The authors declare no conflict of interest

624

625 **References**

626

Alisi A, Carpino G, Oliveira FL, Panera N, Nobili V, Gaudio E (2017) The Role of Tissue Macrophage-Mediated Inflammation on NAFLD Pathogenesis and Its Clinical Implications. *Mediators of inflammation* **2017**: 8162421

627

628

629

Bartel DP (2009) MicroRNAs: target recognition and regulatory functions. *Cell* **136**: 215-233

630

631

Bartel DP (2018) Metazoan MicroRNAs. *Cell* **173**: 20-51

632

633

Basu S, Bhattacharyya SN (2014) Insulin-like growth factor-1 prevents miR-122 production in neighbouring cells to curtail its intercellular transfer to ensure proliferation of human hepatoma cells. *Nucleic acids research* **42**: 7170-7185

634

635

636

637

Becker A, Thakur BK, Weiss JM, Kim HS, Peinado H, Lyden D (2016) Extracellular Vesicles in Cancer: Cell-to-Cell Mediators of Metastasis. *Cancer cell* **30**: 836-848

638

639

640

Berg AH, Scherer PE (2005) Adipose tissue, inflammation, and cardiovascular disease. *Circulation research* **96**: 939-949

641

642

643

Caballero F, Fernandez A, Matias N, Martinez L, Fucho R, Elena M, Caballeria J, Morales A, Fernandez-Checa JC, Garcia-Ruiz C (2010) Specific contribution of methionine and choline in nutritional nonalcoholic steatohepatitis: impact on mitochondrial S-adenosyl-L-methionine and glutathione. *The Journal of biological chemistry* **285**: 18528-18536

644

645

646

647

648

Cai D, Yuan M, Frantz DF, Melendez PA, Hansen L, Lee J, Shoelson SE (2005) Local and systemic insulin resistance resulting from hepatic activation of IKK-beta and NF-kappaB. *Nature medicine* **11**: 183-190

649

650

651

652

Chang J, Nicolas E, Marks D, Sander C, Lerro A, Buendia MA, Xu C, Mason WS, Moloshok T, Bort R, Zaret KS, Taylor JM (2004) miR-122, a mammalian liver-specific microRNA, is processed from hcr mRNA and may downregulate the high affinity cationic amino acid transporter CAT-1. *RNA biology* **1**: 106-113

653

654

655

656

657

Chevillet JR, Kang Q, Ruf IK, Briggs HA, Vojtech LN, Hughes SM, Cheng HH, Arroyo JD, Meredith EK, Gallichotte EN, Pogosova-Agadjanian EL, Morrissey C, Stirewalt DL, Hladik F, Yu EY, Higano CS,

658

659

- 660 Tewari M (2014) Quantitative and stoichiometric analysis of the microRNA content of exosomes.  
661 *Proceedings of the National Academy of Sciences of the United States of America* **111**: 14888-14893
- 662 Esau C, Davis S, Murray SF, Yu XX, Pandey SK, Pear M, Watts L, Booten SL, Graham M, McKay R,  
663 Subramaniam A, Propp S, Lollo BA, Freier S, Bennett CF, Bhanot S, Monia BP (2006) miR-122  
664 regulation of lipid metabolism revealed by in vivo antisense targeting. *Cell metabolism* **3**: 87-98  
665
- 666 Filipowicz W, Bhattacharyya SN, Sonenberg N (2008) Mechanisms of post-transcriptional regulation  
667 by microRNAs: are the answers in sight? *Nature reviews Genetics* **9**: 102-114  
668
- 669 Han KY, Dugas-Ford J, Seiki M, Chang JH, Azar DT (2015) Evidence for the Involvement of MMP14 in  
670 MMP2 Processing and Recruitment in Exosomes of Corneal Fibroblasts. *Investigative ophthalmology*  
671 *& visual science* **56**: 5323-5329  
672
- 673 Han L, Sheng B, Zeng Q, Yao W, Jiang Q (2020) Correlation between MMP2 expression in lung cancer  
674 tissues and clinical parameters: a retrospective clinical analysis. *BMC pulmonary medicine* **20**: 283  
675
- 676 Jo YK, Park SJ, Shin JH, Kim Y, Hwang JJ, Cho DH, Kim JC (2011) ARP101, a selective MMP-2 inhibitor,  
677 induces autophagy-associated cell death in cancer cells. *Biochemical and biophysical research*  
678 *communications* **404**: 1039-1043  
679
- 680 Jopling C (2012) Liver-specific microRNA-122: Biogenesis and function. *RNA biology* **9**: 137-142  
681
- 682 Lotvall J, Valadi H (2007) Cell to cell signalling via exosomes through esRNA. *Cell Adh Migr* **1**: 156-158  
683
- 684 Momen-Heravi F, Bala S, Kodys K, Szabo G (2015) Exosomes derived from alcohol-treated  
685 hepatocytes horizontally transfer liver specific miRNA-122 and sensitize monocytes to LPS. *Scientific*  
686 *reports* **5**: 9991  
687
- 688 Morinaga H, Mayoral R, Heinrichsdorff J, Osborn O, Franck N, Hah N, Walenta E, Bandyopadhyay G,  
689 Pessentheiner AR, Chi TJ, Chung H, Bogner-Strauss JG, Evans RM, Olefsky JM, Oh DY (2015)  
690 Characterization of distinct subpopulations of hepatic macrophages in HFD/obese mice. *Diabetes* **64**:  
691 1120-1130  
692
- 693 Mukherjee K, Ghoshal B, Ghosh S, Chakrabarty Y, Shwetha S, Das S, Bhattacharyya SN (2016)  
694 Reversible HuR-microRNA binding controls extracellular export of miR-122 and augments stress  
695 response. *EMBO reports* **17**: 1184-1203  
696
- 697 Pirola CJ, Fernandez Gianotti T, Castano GO, Mallardi P, San Martino J, Mora Gonzalez Lopez  
698 Ledesma M, Flichman D, Mirshahi F, Sanyal AJ, Sookoian S (2015) Circulating microRNA signature in  
699 non-alcoholic fatty liver disease: from serum non-coding RNAs to liver histology and disease  
700 pathogenesis. *Gut* **64**: 800-812  
701

- 702 Shimoda M, Khokha R (2017) Metalloproteinases in extracellular vesicles. *Biochimica et biophysica*  
703 *acta Molecular cell research* **1864**: 1989-2000  
704
- 705 Shoelson SE, Lee J, Goldfine AB (2006) Inflammation and insulin resistance. *The Journal of clinical*  
706 *investigation* **116**: 1793-1801  
707
- 708 Tan Y, Ge G, Pan T, Wen D, Gan J (2014) A pilot study of serum microRNAs panel as potential  
709 biomarkers for diagnosis of nonalcoholic fatty liver disease. *PloS one* **9**: e105192  
710
- 711 Tang H, He Y, Li L, Mao W, Chen X, Ni H, Dong Y, Lyu F (2019) Exosomal MMP2 derived from mature  
712 osteoblasts promotes angiogenesis of endothelial cells via VEGF/Erk1/2 signaling pathway.  
713 *Experimental cell research* **383**: 111541  
714
- 715 Valadi H, Ekstrom K, Bossios A, Sjostrand M, Lee JJ, Lotvall JO (2007) Exosome-mediated transfer of  
716 mRNAs and microRNAs is a novel mechanism of genetic exchange between cells. *Nature cell biology*  
717 **9**: 654-659  
718
- 719 Wang B, Ding YM, Fan P, Xu JH, Wang WX (2014) Expression and significance of MMP2 and HIF-  
720 1alpha in hepatocellular carcinoma. *Oncology letters* **8**: 539-546  
721
- 722 Wang Y, Liang H, Jin F, Yan X, Xu G, Hu H, Liang G, Zhan S, Hu X, Zhao Q, Liu Y, Jiang ZY, Zhang CY,  
723 Chen X, Zen K (2019) Injured liver-released miRNA-122 elicits acute pulmonary inflammation via  
724 activating alveolar macrophage TLR7 signaling pathway. *Proceedings of the National Academy of*  
725 *Sciences of the United States of America* **116**: 6162-6171  
726
- 727
- 728
- 729
- 730

## Figure legends

731

### **Figure 1 Transfer of miR-122 from hepatic cells to tissue macrophages in MCD diet fed mouse liver**

732

733

**A** Isolation and characterization of Non-Parenchymal Cells (NPCs) from chow diet and MCD diet fed mouse liver. Schematic diagram showing isolation and FACS sorting of NPCs from chow diet fed (Control) vs MCD diet fed mice livers with CD11b (APC) and F4/80 (FITC) gating.

734

735

736

737

**B** Haematoxylin and Eosin stained micrographs of control and MCD diet fed mice liver sections

738

739

**C-D** Hepatic immune cells in MCD diet fed mice show significantly higher levels of internalized miR-122 with respect to control. Relative internalized miR-122 level in sorted RHM cells is shown (C, top panel). As a control, levels of pre-miR-122 (C, middle panel) and internalized miR-16 (C, bottom panel) have also been measured. Relative levels of internalized miR-122 in sorted KC cells is shown (D- top panel, left side). As a control, relative pre-miR-122 (D- bottom panel, left side) and internalized miR-16 (D- top panel, right side) and miR-155 levels (D- bottom panel, right side) have also been shown in the sorted KC cells. miR-155 induction is characteristic of inflammatory response.

740

741

742

743

744

745

746

747

**E-F** Higher levels of internalized miR-122 correlates with increased expression of various pro-inflammatory cytokine mRNAs. Levels of pro-inflammatory cytokines (TNF $\alpha$ , IL-6 and IL1 $\beta$ ) in sorted RHM cells (E) and KC cells (F) from control and MCD diet fed mice livers are shown.

748

749

750

751

All mRNA and miRNA detections were done by RT-qPCR. RT-qPCR detection of cytokine mRNAs and pre-miR-122 was done using specific primers from 200 ng of cellular RNA. RT-qPCR detection of internalized miRNAs and miR-155 was done from 25ng of isolated cellular RNA. Normalization of miR-122, miR-155 and miR-16 were done against U6 snRNA.

752

753

754

755

756 Normalization of precursor miR-122 and cytokine mRNAs were performed in respect to 18S  
757 rRNA levels. Data represents Mean  $\pm$  SD. All images are representative of at least 4  
758 independent mice from each group. For statistical significance, minimum three independent  
759 experiments were considered in each case unless otherwise mentioned and error bars are  
760 represented as mean  $\pm$  S.D. P-values were calculated by utilising Student's t-test. ns:  
761 non-significant, \*P < 0.05, \*\*P < 0.01, \*\*\*P < 0.0001.

762

763 **Figure 2 Extracellular Vesicle mediated transfer of miR-122 from lipid-exposed hepatic**  
764 **cells to tissue macrophages activates them to express pro-inflammatory cytokines**

765 EV associated miR-122 from lipid treated hepatic cells when transferred to recipient  
766 macrophages induce higher levels of proinflammatory cytokine mRNAs. Exosomes were  
767 isolated from different types of hepatic cells treated with 5x cholesterol-lipid concentrate for 4  
768 hours. For the 'w/o cholesterol' sets, equivalent volume of cholesterol-lipid concentrate was  
769 added to the cell supernatant after its collection from the cell culture plates. The 'control' set  
770 represents immune cells to which no EVs have been added. EV treatment was done for  
771 16hours following which recipient cells were lysed and cellular RNA was isolated.

772 **A** Schematic diagram showing experimental procedure described above.

773 **B** Relative levels of exosomal miRNAs secreted by Huh7 cells upon exposure to cholesterol-  
774 lipid concentrate.

775 **C** Relative levels of TNF $\alpha$ , IL-6 and IL-1 $\beta$  in PMA-differentiated U937 cells to which EVs  
776 isolated from cholesterol treated Huh7 cells were added.

777 **D** Relative proinflammatory cytokine mRNA levels in murine primary macrophages incubated  
778 with EVs isolated from cholesterol treated primary hepatocytes.

779 **E** Internalized miR-122 (left panel) and miR-16 (right panel) in primary macrophages of  
780 experiment described in (D).

781 **F** Relative levels of TNF $\alpha$  mRNA (top panel), IL-6 mRNA (middle panel) and IL-1 $\beta$  mRNA  
782 (bottom panel) in recipient RAW 264.7 monocytes incubated with EVs from cholesterol  
783 treated Hepa1-6 cells expressing miR-122 (miR-122 expression plasmid pmiR-122  
784 transfected).

785 **G** Inhibition of internalized miR-122 in recipient macrophages leads to reversal of  
786 proinflammatory cytokine expression. EVs isolated from untreated (w/o cholesterol) and 5x  
787 cholesterol-lipid concentrate treated (w/cholesterol) Hepa1-6 cells (pmiR-122 transfected)  
788 were added to RAW 264.7 cells prior-transfected with anti-miR-122 oligos (Anti-miR-122 w/o  
789 cholesterol, anti-miR-122 w/ cholesterol). mRNA levels of TNF- $\alpha$  (top panel), IL-6 (middle  
790 panel) and IL-1 $\beta$  (bottom panel) were detected by RT-qPCR.

791 **H-I** Presence of miR-122 in macrophage cells induces a pro-inflammatory phenotype.  
792 Induction of miR-122 expression in RAW264.7 leads to elevated levels of proinflammatory  
793 cytokine mRNAs. Tetracycline repressor expressing RAW264.7 cells were transfected with  
794 inducible miR-122 expressing plasmids. 400 ng/ml of Doxycycline was used to induce miR-  
795 122 expression. mRNA levels of TNF- $\alpha$ , IL-6 and IL-1 $\beta$  detected by RT-qPCR in cells  
796 harvested at indicated time points after Dox addition have been shown here (H). Relative  
797 miR-122 levels in RAW264.7 at various time points since DOX addition (I).

798 All mRNA and miRNA detections were done by RT-qPCR. RT-qPCR detection of cellular  
799 miRNAs was done from 25 ng of cellular RNA. RT-qPCR detection of EV miRNAs was done  
800 from 100 ng of isolated EV RNA. Normalization of miR-122 and miR-16 were done with  
801 respect to U6 snRNA. Normalization of precursor miR-122 and cytokine mRNAs were done  
802 with respect to 18S rRNA. Data represents Mean  $\pm$  SD. (B-I) N= 3 replicates. P-values were

803 calculated by utilising Student's t-test. ns: non-significant, \*P < 0.05, \*\*P < 0.01, \*\*\*P <  
804 0.0001.

### 805 **Figure 3 MMP2 dependent entry of EV in recipient cells**

806 **A-C** Experimental scheme is shown in panel A. Donor Huh7 cells were transfected with cy3-  
807 labelled miR-122 oligonucleotides and siMMP2 before the EVs were isolated. The quantity  
808 and size distribution of the EVs were characterized by nano particle tracking analysis (B).  
809 Recipient HeLa cells were seeded on the gelatin coated coverslips at the lower chamber of  
810 the 24 well plates. Bottom of 0.4µM pore containing inserts were coated with diluted growth  
811 factor reduced matrigel (3mg/ml) and incubated in 37°C incubator for 30-45 min. After  
812 incubation, EVs were added into the inserts with the presence or absence of ARP101 or  
813 DMSO or rMMP2 and then it was kept for incubation for 24 hrs (A). Next day, after cell  
814 fixation, permeabilization and staining for β-tubulin cells were imaged (C).

815 **D** Donor Huh7 cells were transfected with CD63GFP, siCon and siMMP2 and EVs were  
816 isolated. The number of CD63GFP transfer from donor cell exosome to recipient HeLa cell  
817 was also quantified by counting green dots of CD63 from three different sets, 5 fields/set, 5  
818 cells/field. EVs from SiCon treated cells were used as control. ARP101 and rMMP2 were  
819 added along with EVs from CD63GFP expressing cells in respective condition.

820 **E-G** The number of miR-122 transfer from donor cell exosome to recipient HeLa cell was  
821 also quantified by counting red dots of cy3-miR-122 from three different sets, 5 fields/set, 5  
822 cells/field (E). The number of CD63GFP transfer from donor cell EVs to recipient HeLa cell  
823 was also quantified by counting green dots of CD63 from three different sets, 5 fields/set, 5  
824 cells/field (F). The downregulation of MMP2 expression was observed when siMMP2 was  
825 transfected to donor cells by western blotting (G).

826 For statistical significance, minimum three independent experiments were considered in  
827 each case unless otherwise mentioned and error bars are represented as mean ± S.E.M.



828 P-values were calculated by utilising Student's t-test. ns: non-significant, \*P < 0.05, \*\*P <  
829 0.01, \*\*\*P < 0.0001. Scale bars in panel C and D are of 10  $\mu$ m length .

830 **Figure 4 Functional transfer of miR-122 between hepatic cells requires MMP2 activity.**

831 **A-B** ARP101 inhibits the transfer of miR-122 containing EVs from donor cell to recipient  
832 cells. The transfer of EVs from hepatic cell lines were checked by using a specific MMP-2  
833 inhibitor ARP101 (12.5 $\mu$ M/well). Huh7 (A) and HeLa (B) cells were chosen and transfected  
834 with miR-122 expressing pmiR-122 or anti-miR-122 oligoes and EVs were isolated. HepG2  
835 cells were taken as recipient cell. To check the transfer, transwell inserts (0.4  $\mu$ M, SPL) were  
836 taken and 100  $\mu$ l 3mg/ml diluted matrigel were coated and solidified previously. In the lower  
837 chamber, HepG2 cells were seeded in complete DMEM media with 10% FCS. EVs were  
838 added in the medium in the inserts and incubated for 30 min in 37°C incubator. Serum free  
839 DMEM was added on to the inserts with ARP101. In control sets, same amount of DMSO  
840 (v/v) was added. This was then kept for 24 hrs in incubator. Next day, RNA was isolated by  
841 using Trizol™ RNA isolation method from HePG2 cells and cDNA was synthesized followed  
842 by real time PCR for miR-122 by using miR-122 primers. Normalization was done with  
843 respect to U6 snRNA. Data represents Mean  $\pm$  SD.

844 **C-F** Luciferase activity showed the repression of miR-122 reporter in recipient cells by  
845 transferred miR-122 from donor cells. The fold repression is the ratio of normalized  
846 expression levels obtained with RL-con and RL miR-122 reporter having one miR-122  
847 perfect binding sites (C and D). In similar experiments described in A and B, the repressive  
848 activities in presence or absence of ARP101 were measured in HepG2 cells that don't  
849 express miR-122 otherwise. Huh7, HepG2 and HeLa cells were overexpressed with miR-  
850 122 and exosomes were isolated and added to the matrigel coated 0.4micron inserts as  
851 previously. Recipient HepG2 cells were transfected with either RL-con or RL-per-miR-122  
852 plasmids in parallel sets. To detect fold repression in HepG2, 10<sup>6</sup> cells in a 10 cm<sup>2</sup> well were  
853 transfected with 150 ng of each of the plasmids. Normalisation was done with a Firefly (FF)

854 luciferase construct which was co-transfected along with the RL constructs ( $1\mu\text{g}$  for  $1 \times 10^6$   
855 cells) after 24 h of transfection, cells were then spilted and seeded in the lower chamber of  
856 the transwell insert. ARP101 was added as described earlier. The whole set was incubated  
857 for 24 hrs again. Data represents Mean  $\pm$  SD.

858 **G** miR-122 expression was checked by ARP101 in donor cells. Huh7 cells were transfected  
859 with pmiR-122 and seeded in Matrigel with or without MMP2 inhibitor ARP101 in 24 well  
860 plate and incubated for 24 hrs. Cells were isolated from Matrigel and RNA was isolated  
861 followed by cDNA and Real time PCR for miR-122 and normalization of value obtained were  
862 done against U6 snRNA. Data represents Mean  $\pm$  SD.

863 **Figure 5 Presence of MMP2 on the Extracellular Vesicles (EVs) isolated from different**  
864 **hepatic and non-hepatic cells.**

865 A Gelatin Zymography reveals the presence of functional MMP2 in EVs isolated from hepatic  
866 cells. Extracellular vesicles or Exosomes were isolated from hepatic Huh7 cells transfected  
867 with or without miR-122 expressing plasmid pmiR-122 or pCIneo control plasmid. Anti-miR-  
868 122 treatment was also done in separate set cells. Cell lysates and EV extract (100ng  
869 protein each) were electrophoresed in 8% SDS-polyacrylamide gel containing 1 mg/ml  
870 gelatin under non-reducing conditions.

871 B Presence of MMP2 in EVs isolated from hepatic and non hepatic cells (Huh7 & HeLa).  
872 Cells were transfected either with miR-122 expressing plasmid pmiR-122 or pCIneo vector.  
873 Extract of cells or isolated EVs (100 ng each) were then electrophoresed in 10% SDS-  
874 polyacrylamide gel.

875 C Effect of Proteinase K (PK) treatment ( $20\mu\text{g}/\text{ml}$ ) on EV associated Alix, MMP2 and HuR  
876 protein. Isolated EVS were treated with PK and after the incubation reaction was stopped  
877 and analyzed on 10% SDS-PAGE and western blotted.

878 D-E Effect of MMP14 down regulation on MMP2 association with EVs. Huh7 cells were  
879 transfected with siRNAs specific to MMP14 or control siRNA and the cellular and EV  
880 associated levels of MMP14 and MMP2 were detected by western blot in respective sample  
881 (D). A suggested model of MMP14 mediated MMP2 recruitment of MMP2 to EVs (E)

882 **Fig. 6: Inhibition of MMP2 affect transfer of pro-inflammatory signal across the hepatic**  
883 **cell boundary**

884 MMP2 facilitates the miR-122 transfer to macrophage that leads to elevated levels of  
885 various pro-inflammatory cytokine mRNAs. Scheme of the experiment has been shown in  
886 panel A. Huh7 was transfected with control vector or pmiR-122 and EVs were isolated. Here  
887 RAW264.7 cells were taken as recipient cell. To check the transfer, transwell inserts (0.4  
888 micron, SPL) were taken and 100  $\mu$ l (3mg/ml) diluted matrigel were coated and solidified  
889 previously. In the lower chamber, RAW264.7 cells were seeded in complete RPMI media  
890 with 10% FCS. Then RAW264.7 cells were activated using LPS (1mg/ml) for 4 hrs.  
891 Exosomes were added on the inserts and incubated for 30 min in 37°C incubator. Serum  
892 free DMEM was added on to the inserts with ARP101 (12.5 $\mu$ M/well). In control sets, same  
893 amount of DMSO (v/v) was added. This was then kept for 24 hrs in incubator. Next day,  
894 inserts were removed and media from the lower chamber was discarded and RNA was  
895 isolated by using Trizol™ RNA isolation method. cDNA was synthesized followed by real  
896 time PCR for pro inflammatory (IL-1 $\beta$  and TNF- $\alpha$ ) cytokines and miR-122 (B). Normalization  
897 was done with respect to 18S rRNA and U6 snRNA respectively. Data represents Mean  $\pm$   
898 SD.

899 **C-D** Relative internalized miR-122 levels to non-parenchymatous hepatic cells in presence  
900 and absence of ARP101. The scheme of the experiment has been shown in panel C. EVs  
901 isolated from miR-122 expressing Hepa1-6 cells, were injected through the tail vein every  
902 alternate day for three days and mice sacrificed the next day after the third injection. Equal  
903 volume of PBS was administered as the control. Non-prenchymatous hepatic cells were

904 isolated. Low miR-122 level was detected when MMP2 inhibitor was applied. Normalization  
905 was done with respect to U6 snRNA. Data represents Mean  $\pm$  SD (D). Cytokine mRNA  
906 levels in isolated non-parenchymatous hepatic cells have been shown here. mRNA levels  
907 were detected by RT-qPCR. Normalization was done with respect to 18S. Data represents  
908 Mean  $\pm$  SD (D).

909 E A model of EV-mediated activation of resident macrophage in liver. The miR-122 containing  
910 EVs released by activated hepatocytes digest the matrix by associated MMP2 and get  
911 transferred to non-parenchymatous hepatic cells to activate them to express the pro-  
912 inflammatory cytokines-a process get inhibited by ARP101, the MMP2 inhibitor.

913 For statistical significance, minimum three independent experiments were considered in  
914 each case unless otherwise mentioned and error bars are represented as mean  $\pm$  S.E.M.  
915 P-values were calculated by utilising Student's t-test. ns: non-significant, \*P < 0.05, \*\*P <  
916 0.01, \*\*\*P < 0.0001.

917

918

919

920 **Supplementary Figure S1 Internalization of external miR-122 by hepatic immune cells**  
921 ***in vivo* elevates expression of proinflammatory cytokine mRNAs.**

922 **A-D** Schematic diagram to show the tail vein injection schedule in mice (A).  $1 \times 10^9$  EVs  
923 isolated from miR-122 expressing Hepa1-6 cells were injected through the tail vein as per  
924 the given schedule for each mice. Equal volume of PBS was administered as the control.  
925 Mice were sacrificed on day 5 and non parenchymatous hepatic cells isolated from the liver.  
926 Cytokine mRNA (TNF- $\alpha$  and IL-1 $\beta$ ) levels in non parenchymatous hepatic cells isolated from  
927 EV-injected and control (PBS) injected mice have been shown here (B). Relative internalized  
928 miR-122 levels in non parenchymatous hepatic cells are shown (C). Levels of circulatory  
929 miR-122 and miR-16 in serum RNA of EV and PBS injected mice are shown (D).

930 All mRNA and miRNA detections were done by RT-qPCR. RT-qPCR detection of cellular  
931 miRNAs was done from 25 ng of cellular RNA. RT-qPCR detection of EV miRNAs was done  
932 from 100 ng of isolated EV RNA. Normalization of miR-122 and miR-16 were done with  
933 respect to U6 snRNA. Normalization of precursor miR-122 and cytokine mRNAs were done  
934 with respect to 18S rRNA. Data represents Mean  $\pm$  SD. (A) N= 3 replicates. (B-D) All data  
935 are representative of at least 4 independent mice from each group. For detection of  
936 circulatory miRNA (D) serum was isolated from 3 mice of each group. For statistical  
937 significance, minimum three independent experiments were considered in each case unless  
938 otherwise mentioned and error bars are represented as mean  $\pm$  S.D. P-values were  
939 calculated by utilising Student's t-test. ns: non-significant, \*P < 0.05, \*\*P < 0.01, \*\*\*P <  
940 0.0001.

941 **Supplementary Figure S2 MMP2 facilitates movement of EVs across the extracellular**  
942 **matrix**

943 **A** The diffusion rate measurement assay done with Huh7 released EVs pretreated with  
944 rMMP2 or ARP101 as MMP2 inhibitor. EVs were isolated from culture supernatant of Huh7

945 cells ( $1 \times 10^7$  Cells). The EVs were then spotted on a well formed in middle of a 35mm Petri  
946 disc layered with 2mm thick gelatine matrix. After 30 minutes the reaction were stopped and  
947 the gelatin matrix were stained with Brilliant Blue to visualize the diffusion front of the EVs  
948 through the matrix.

949 **B-C** The diffusion boundary of EVS in presence and absence of MMP inhibitor ARP101 and  
950 rMMP2. The representative plate photographs with marked boundary postions have been  
951 shown (B). The diffusion rate calculated from the distance travelled in mm in unit time has  
952 been plaotted based on three measurements (n=3) (C).

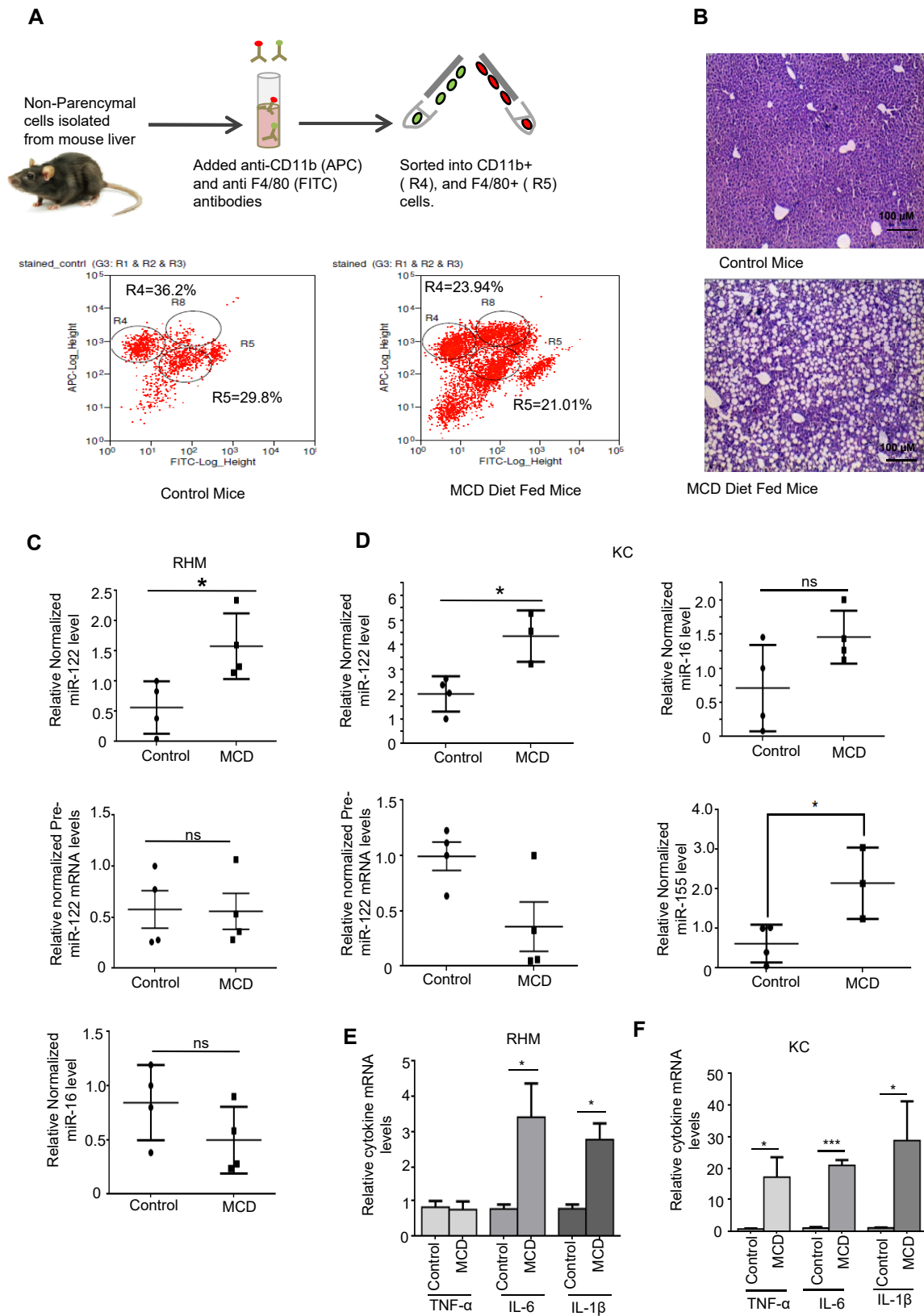
953 **D-E** MMP2 also facilitate uptake of EVs in recipient cells. The CD63-GFP positive EV  
954 transfer from donor cell to recipient HeLa cell grown without the matrigel. The experiments  
955 were done in presence and absence of MMP2 inhibitor ARP101 and rMMP2 (D). The  
956 quantification were done microscopically and plotted (E) The total number was also  
957 quantified by counting green dots of CD63 from three different sets, 5 fields/set, 5 cells/field.

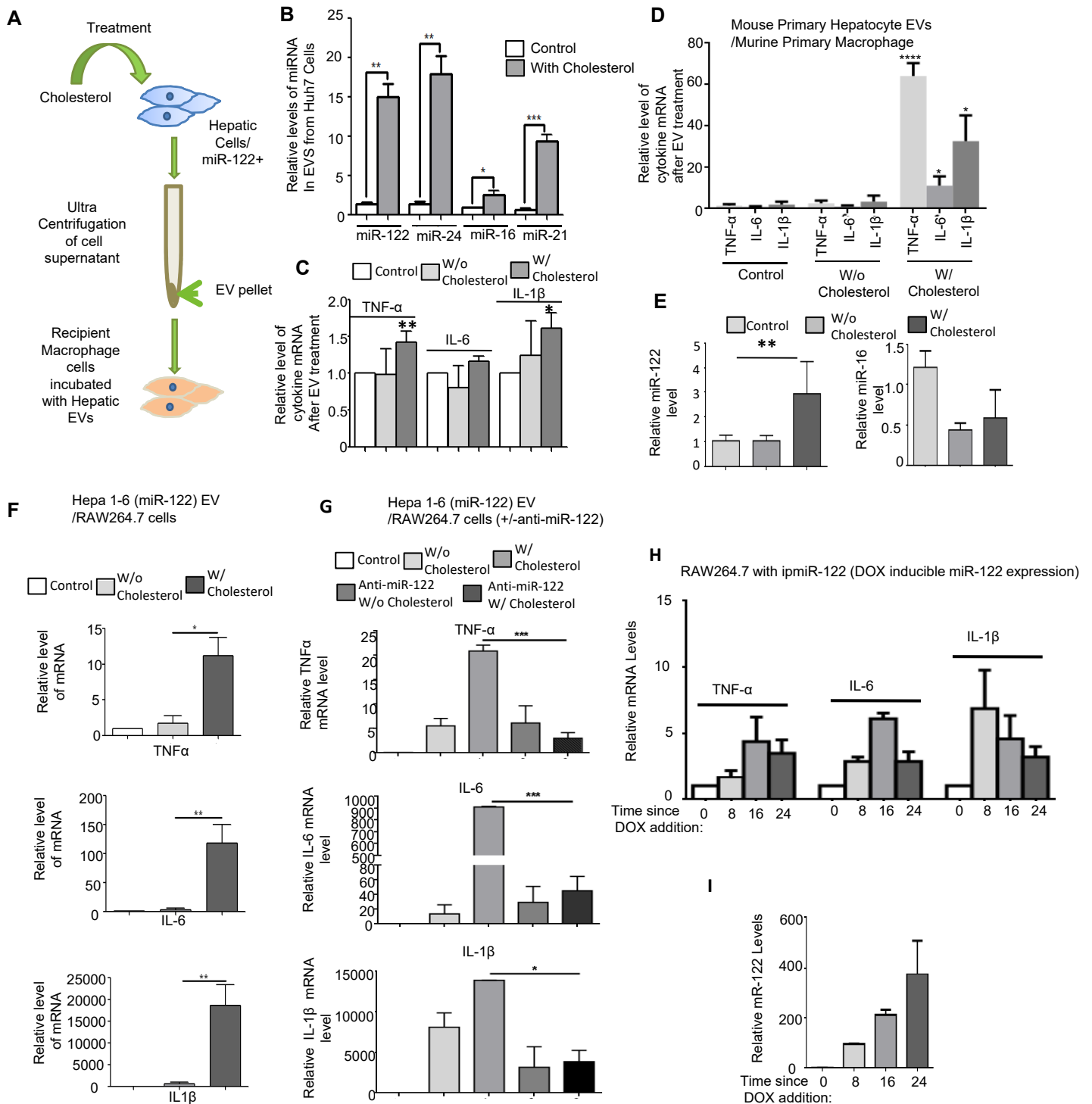
958 For statistical significance, minimum three independent experiments were considered in  
959 each case unless otherwise mentioned and error bars are represented as mean  $\pm$  S.E.M.  
960 P-values were calculated by utilising Student's t-test. ns: non-significant, \*P < 0.05, \*\*P <  
961 0.01, \*\*\*P < 0.0001.

962

963

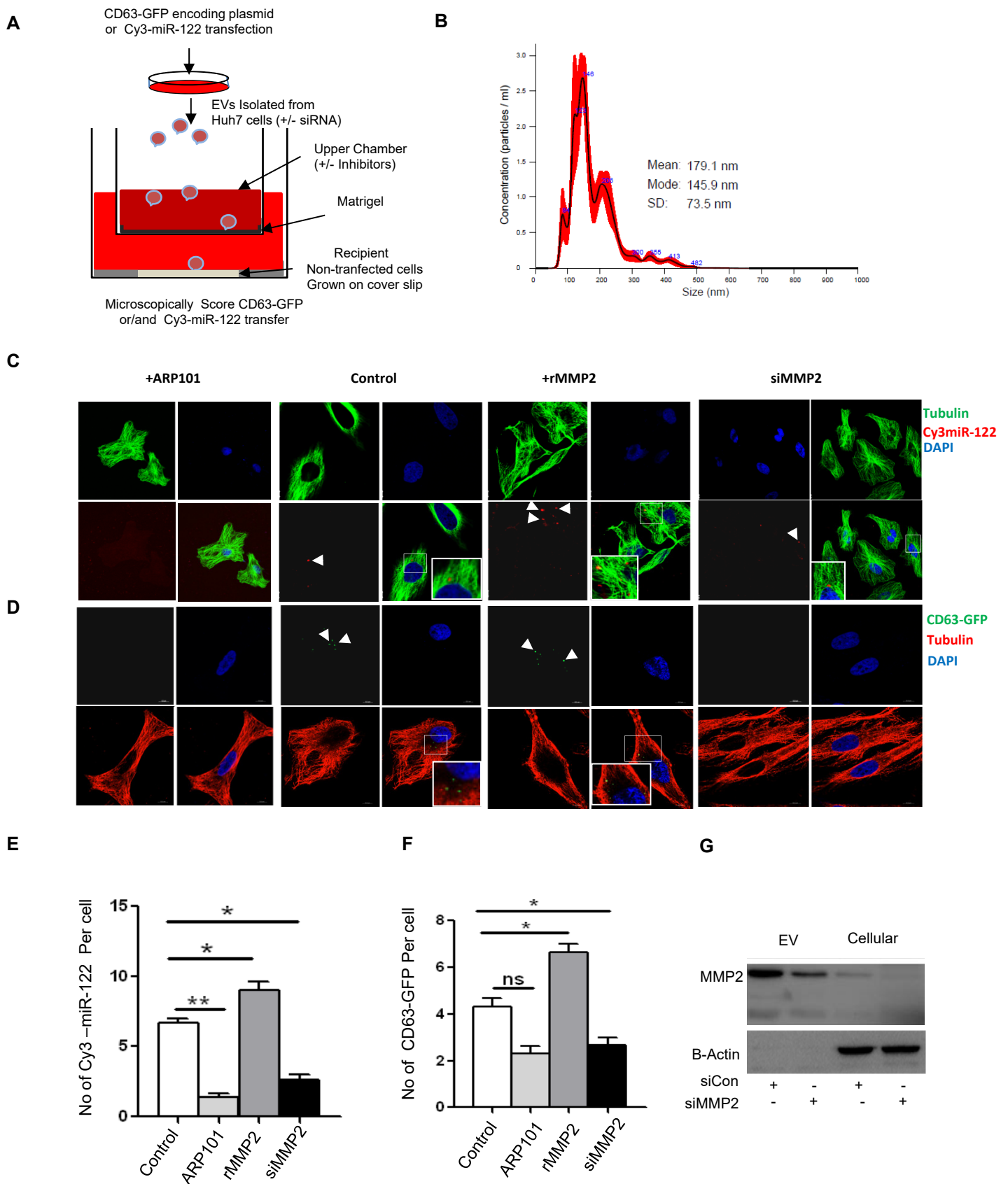
# Figure 1

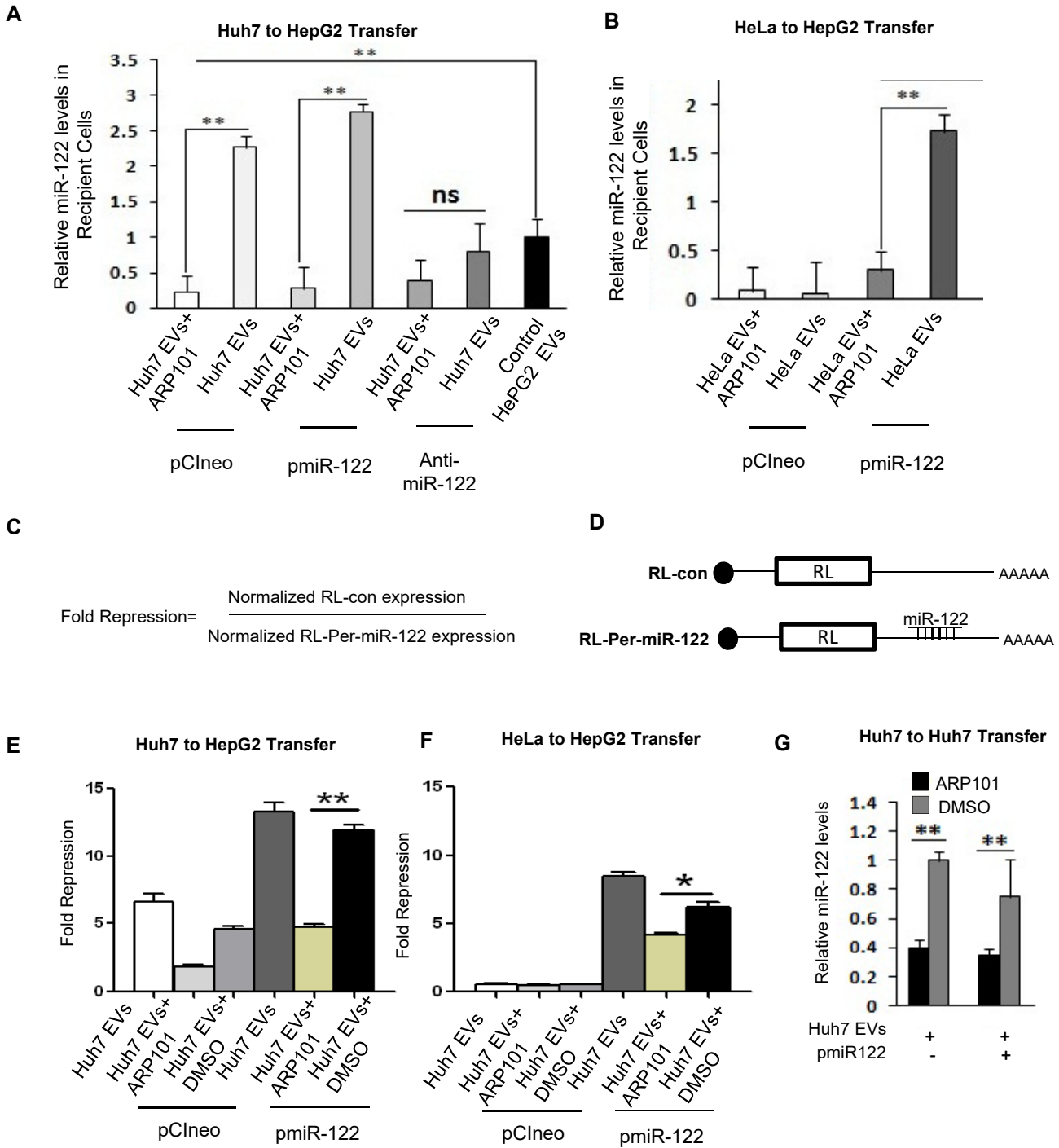




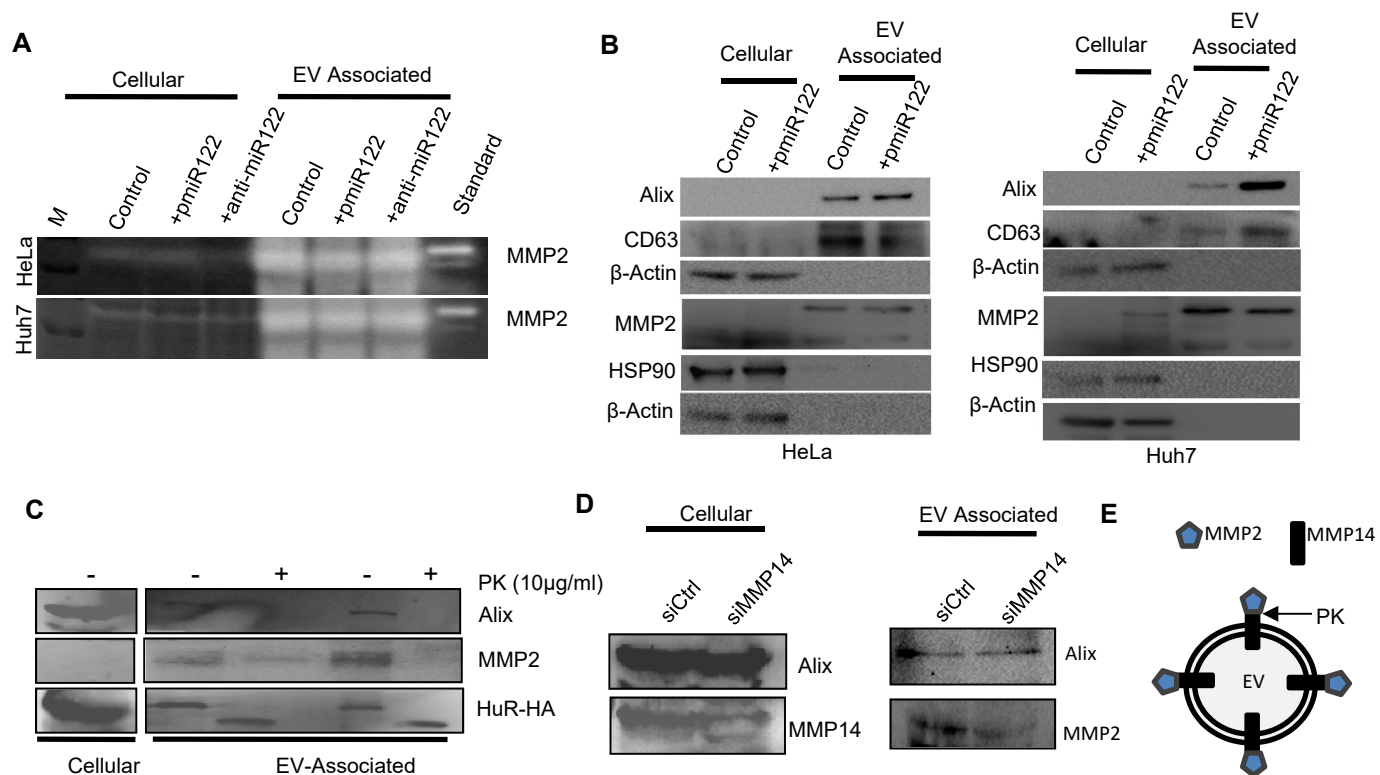


## Figure 3





## Figure 5



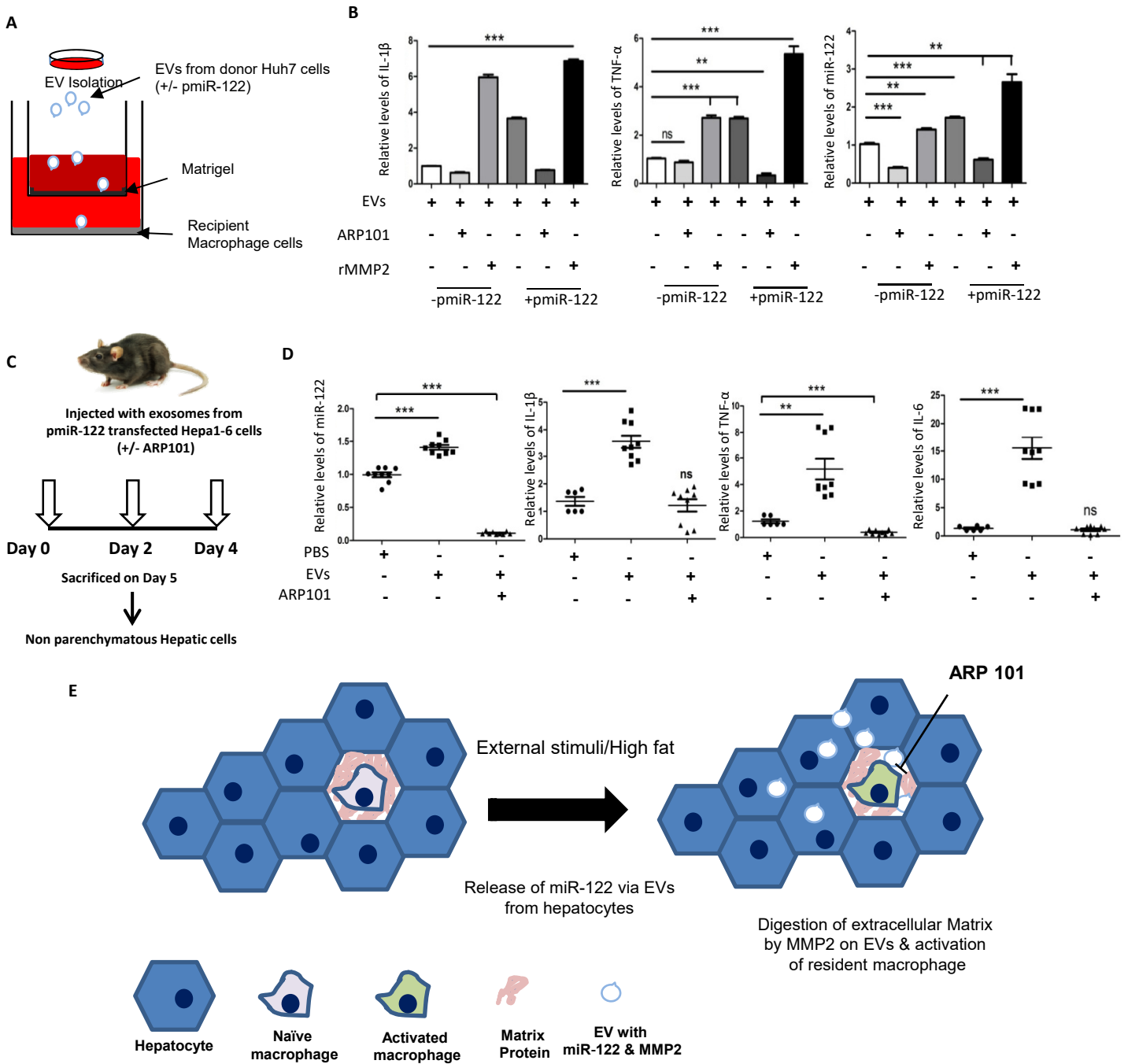


## Figure S1

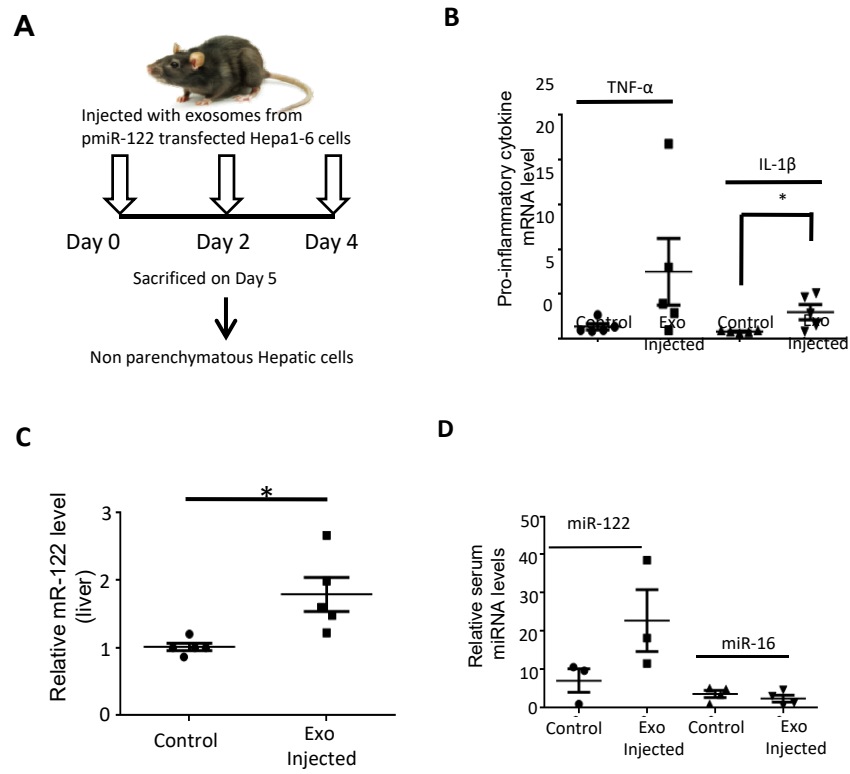


## Figure S2

